The Question of Recharge to the Deep Thermal Reservoir Underlying the Geysers and Hot Springs of Yellowstone National Park

H

By Robert O. Rye and Alfred H. Truesdell

Chapter H *of*
Integrated Geoscience Studies in the Greater Yellowstone Area—Volcanic, Tectonic, and Hydrothermal Processes in the Yellowstone Geoecosystem
Edited by Lisa A. Morgan

U.S. Geological Survey Professional Paper 1717

U.S. Department of the Interior
U.S. Geological Survey

Contents

Figures

Tables

The Question of Recharge to the Deep Thermal Reservoir Underlying the Geysers and Hot Springs of Yellowstone National Park

By Robert O. Rye[1] and Alfred H. Truesdell[2]

Abstract

The extraordinary number, size, and unspoiled beauty of the geysers and hot springs of Yellowstone National Park (the Park) make them a national treasure. The hydrology of these special features and their relation to cold waters of the Yellowstone area are poorly known. In the absence of deep drill holes, such information is available only indirectly from isotope studies. The δD-$\delta^{18}O$ values of precipitation and cold surface-water and ground-water samples are close to the global meteoric water line (Craig, 1961). δD values of monthly samples of rain and snow collected from 1978 to 1981 at two stations in the Park show strong seasonal variations, with average values for winter months close to those for cold waters near the collection sites. δD values of more than 300 samples from cold springs, cold streams, and rivers collected during the fall from 1967 to 1992 show consistent north-south and east-west patterns throughout and outside of the Park, although values at a given site vary by as much as 8 ‰ from year to year. These data, along with hot-spring data (Truesdell and others, 1977; Pearson and Truesdell, 1978), show that ascending Yellowstone thermal waters are modified isotopically and chemically by a variety of boiling and mixing processes in shallow reservoirs. Near geyser basins, shallow recharge waters from nearby rhyolite plateaus dilute the ascending deep thermal waters, particularly at basin margins, and mix and boil in reservoirs that commonly are interconnected. Deep recharge appears to derive from a major deep thermal-reservoir fluid that supplies steam and hot water to all geyser basins on the west side of the Park and perhaps in the entire Yellowstone caldera. This water ($T \geq 350°C$; $\delta D = -149 \pm 1$ ‰) is isotopically lighter than all but the farthest north, highest altitude cold springs and streams and a sinter-producing warm spring ($\delta D = -153$ ‰) north of the Park.

Derivation of this deep fluid solely from present-day recharge is problematical. The designation of source areas depends on assumptions about the age of the deep water, which in turn depend on assumptions about the nature of the deep thermal system. Modeling, based on published chloride-flux studies of thermal waters, suggests that for a 0.5- to 4-km-deep reservoir the residence time of most of the thermal water could be less than 1,900 years, for a piston-flow model, to more than 10,000 years, for a well-mixed model. For the piston-flow model, the deep system quickly reaches the isotopic composition of the recharge in response to climate change. For this model, stable-isotope data and geologic considerations suggest that the most likely area of recharge for the deep thermal water is in the northwestern part of the Park, in the Gallatin Range, where major north-south faults connect with the caldera. This possible recharge area for the deep thermal water is at least 20 km, and possibly as much as 70 km, from outflow in the thermal areas, indicating the presence of a hydrothermal system as large as those postulated to have operated around large, ancient igneous intrusions. For this model, the volume of isotopically light water infiltrating in the Gallatin Range during our sampling period is too small to balance the present outflow of deep water. This shortfall suggests that some recharge possibly occurred during a cooler time characterized by greater winter precipitation, such as during the Little Ice Age in the 15th century. However, this scenario requires exceptionally fast flow rates of recharge into the deep system.

For the well-mixed model, the composition of the deep reservoir changes slowly in response to climate change, and a significant component of the deep thermal water could have recharged during Pleistocene glaciation. The latter interpretation is consistent with the recent discovery of warm waters in wells and springs in southern Idaho that have δD values 10–20 ‰ lower than the winter snow for their present-day high-level recharge. These waters have been interpreted to be Pleistocene in age (Smith and others, 2002). The well-mixed model permits a significant component of recharge water for the deep system to have δD values less negative than –150 ‰ and consequently for the deep system recharge to be closer to the caldera at a number of possible localities in the Park.

[1]U.S. Geological Survey, Box 25046, Mail Stop 963, Denver Federal Center, Denver, CO 80225.

[2]700 Hermosa Way, Menlo Park, CA 94025.

Introduction

Extraordinary geysers, hot springs, and fumaroles are distributed widely in Yellowstone National Park (the Park), and they constitute one of its major attractions. Public law (The Geothermal Steam Act of 1970 (30 U.S.C. 1001–1025) as amended by Section 28 in 1988) requires that significant thermal features in the Park be protected from the effects of exploration and exploitation for geothermal energy outside of the Park—determination of possible effects are to be based on scientific evidence from monitoring studies by the U.S. Geological Survey. For the purposes of this act, Yellowstone National Park is considered to be a single significant geothermal system, and it is protected in its entirety.

Extensive scientific study of the thermal areas of Yellowstone National Park began with the Hayden Expedition of 1871 (Hayden, 1872) and continued with the geochemical studies of Gooch and Whitfield (1888) and Allen and Day (1935). Since 1960, the U.S. Geological Survey has been active in the study of Yellowstone, with topographic and geologic mapping and geophysical, geothermal, and volcano hazard studies. For a bibliography of these studies from 1965 to 1986, see Bargar and Dzurisin (1986); also see the review by Fournier (1989) and investigations reported in Sorey (1991), Rye and Truesdell (1993), and other papers in this volume. Initial studies of the hydrothermal system(s) in Yellowstone concentrated on the surface thermal features—their character, chemistry, and output. In 1967, as part of a study to understand the geochemistry and hydrology of the thermal areas, we began isotopic studies of cold waters around the geyser basins in an attempt to locate the recharge area(s) for the thermal waters. Chemical and isotopic modeling (Truesdell and others, 1977) indicated that probably all of the hot-spring and geyser basins on the west side of the Yellowstone caldera are underlain by deep meteoric water of constant isotopic and chemical composition. This deep water is modified isotopically and chemically as it cools by boiling and mixing with local cold waters. The recharge area(s) for the deepest parts of the Yellowstone system have not been located. The purpose of this paper is to compare the isotopic compositions of deep thermal-reservoir waters indicated by analyses of hot-spring, geyser and research-well waters (Truesdell and others, 1977) with the compositions of meteoric waters, for the purpose of constraining the source(s) of recharge for the deep waters. A unique solution is not possible because the age of the deep water is not known. If the deep thermal water in the Yellowstone geothermal system is Holocene in age, the most likely area for its meteoric water recharge is in the Gallatin Range in and northwest of the Park. However, if a component of the deep water was recharged during Pleistocene glaciation and if the deep reservoir is well mixed, the recharge area could be multiple localities within the Park, close to the caldera.

Thermal Features of Yellowstone National Park

The areal distribution of active thermal areas in the Park and their relationships to surface drainage and major geologic and topographic features are shown in figure 1. Most of the active thermal areas are (1) in the 0.6-Ma Yellowstone caldera, close to the outer margin (for example, Hot Spring Basin and Washburn Hot Springs) and in the topographically low area near the two resurgent domes (for example, Upper and Lower Geyser Basins) or (2) along north-south-trending faults that extend outside the caldera (for example, Norris and Heart Lake Geyser Basins). Geophysical evidence indicates that an active magma system underlies much of the Yellowstone caldera at depths of about 5–6 km, and it currently produces inflation and deflation of the area (Eaton and others, 1975; Dzurisin and Yamashita, 1987; Dzurisin and others, 1990; Smith and Rubin, 1994; Pierce and others, 1997; Wicks and others, 1999; Pierce and others, this volume).

A variety of thermal features is present in individual basins. In general, alkaline-chloride hot springs are in basins on the west side of the caldera, where one would expect to find cold-water springs. These alkaline-chloride springs deposit thick mounds and terraces of silica on glacial till, welded tuff, and rhyolite. In areas where boiling water does not emerge at the surface, H_2S in the steam that separates from the water commonly oxidizes and forms H_2SO_4 at the surface, and it produces acid-sulfate pools and mud pots. Small travertine-producing springs are present at the margins of geyser basins in which CO_2-charged waters cool by mixing with cold ground water before they have a chance to boil. The thermal features in the east side of the Park have little water discharge and typically consist of fumaroles surrounded by sulfur and steam-heated pools of acid-sulfate water containing little chloride. Because this area is higher than the adjacent valleys, the water table seldom intersects the surface. However, recent studies indicate that there is discharge of chloride-rich waters into Yellowstone Lake from sublacustrine vents (Balistrieri and others, this volume). Large travertine deposits outside of the caldera, such as those at Mammoth Hot Springs and adjacent to the Snake River, occur at the low-temperature margins of the Yellowstone system where thermal fluids flow through thick limestone sequences.

Figure 1. Sketch map of Yellowstone National Park (dashed dot-dot line) showing general locations of geyser basins (dark gray) and their relation to the Yellowstone caldera (heavy black line), important north-south faults (dot dashed line), resurgent domes (diagonal pattern), surface drainage (fine lines), and selected topographic and physiographic features (text and wavy pattern for lakes). Also shown are location of Mammoth and Old Faithful (large white dots), the Continental Divide (open dotted line), roads (short dashed line), and State boundaries (thin dashed lines). Caldera outline, resurgent domes, and faults generalized from Christiansen (1984).

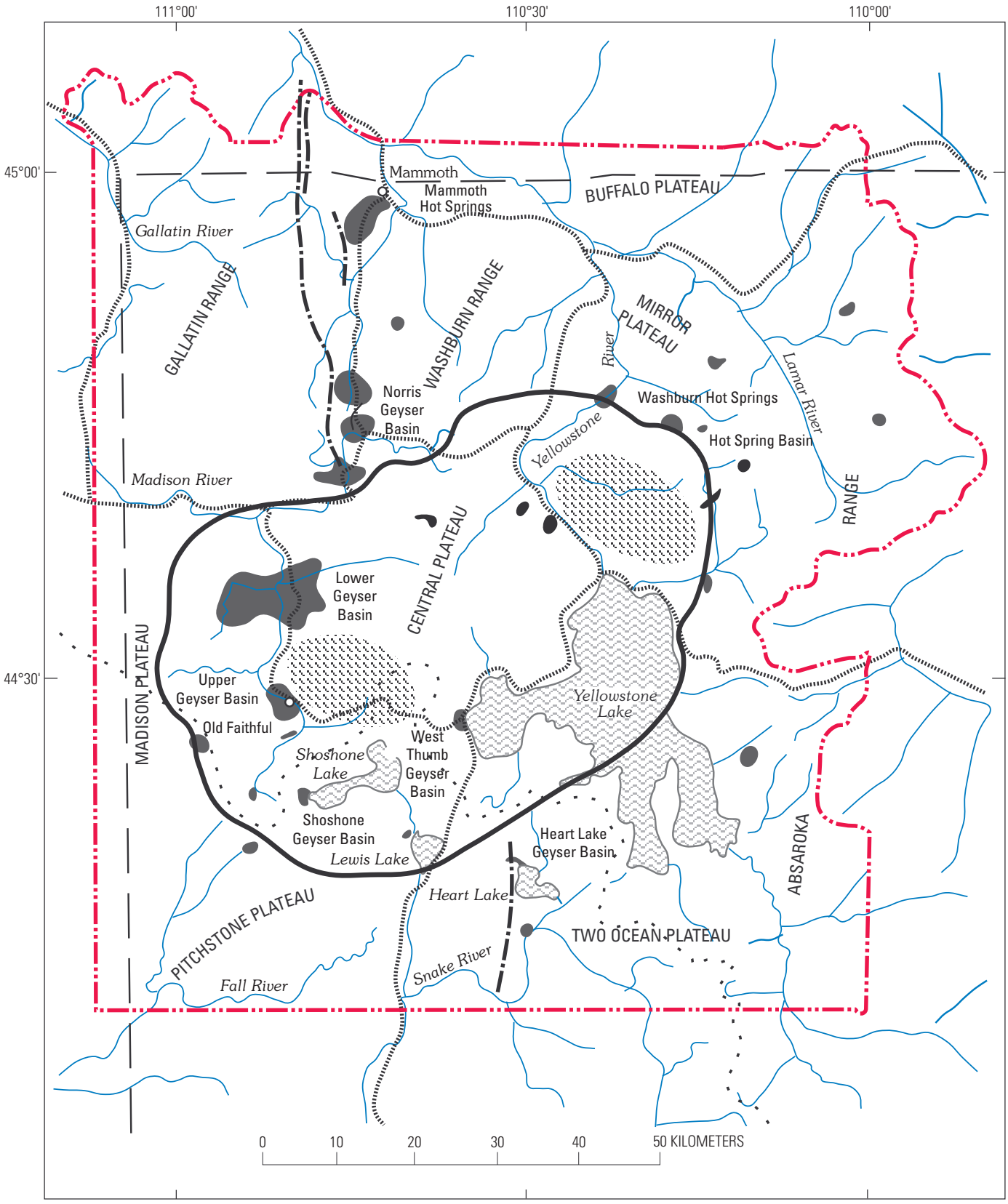
111°00'
110°30'
110°00'
45°00'
44°30'
Mammoth
Mammoth Hot Springs
BUFFALO PLATEAU
Gallatin River
GALLATIN RANGE
WASHBURN RANGE
MIRROR PLATEAU
Yellowstone River
Lamar River
Norris Geyser Basin
Washburn Hot Springs
Hot Spring Basin
Madison River
CENTRAL PLATEAU
RANGE
Lower Geyser Basin
MADISON PLATEAU
Upper Geyser Basin
Old Faithful
Yellowstone Lake
West Thumb Geyser Basin
Shoshone Lake
Shoshone Geyser Basin
Lewis Lake
Heart Lake Geyser Basin
ABSAROKA
Heart Lake
PITCHSTONE PLATEAU
TWO OCEAN PLATEAU
Snake River
Fall River
0 10 20 30 40 50 KILOMETERS

Recognition of a Deep-Water Component in the Thermal System: Comparison of δD of Water from Drill Holes and Thermal Springs

Early isotope studies showed that essentially all of the thermal waters in Yellowstone Park and elsewhere in the world were derived from meteoric water (Craig and others, 1956). Hundreds of additional samples from Yellowstone and other thermal areas throughout the world have been analyzed, and that conclusion still holds, with few exceptions. In order to better understand the geochemistry and hydrodynamics of the thermal areas, in 1967 we began a search for the recharge areas for the thermal water in the Yellowstone geyser basins. At that time, we assumed that the hot springs in each basin were recharged locally by water from the surrounding rhyolite plateaus. Analyses of water collected from shallow (65–332 m depth) research holes drilled in 1967 and 1968 required us to abandon that assumption. The δD values of waters from drill holes and nearby hot-water springs and local meteoric water from Lower, Norris, and Shoshone Geyser Basins are summarized in table 1. The striking feature of the data in table 1 is that δD values of waters from hot springs and drill holes were more negative than those of local meteoric waters. For example, the δD values of water from drill holes at Norris and Lower Geyser Basins were –146 to –151 ‰, whereas those of local meteoric water were –140 to –145 ‰. Recognition of this difference led to modeling of the δD of thermal waters in terms of isotope effects due to boiling and mixing (Truesdell and others, 1977). The results of that modeling for Norris Geyser Basin are illustrated in figure 2. The boiling and mixing model enabled interpretation of the measured δD of spring waters in terms of δD of deep water prior to boiling and (or) mixing. The deep thermal waters mix with cool water from local sources in shallow reservoirs, and these mixtures boil to produce the chemical and isotopic compositions of the surface thermal waters. Because most boiling and mixing occurs in shallow aquifers, the δD values of waters recovered from drill holes approximate the primary compositions of thermal waters prior to boiling and mixing. This modeling indicated that hot springs in the Norris Geyser Basin have a deep-water component that was derived from meteoric water having a δD significantly lower than that of present local meteoric waters. Truesdell and others (1977) showed that the compositions of thermal waters at Lower and Shoshone Geyser Basins also are consistent with derivation from the same deep water of δD = –148 to –150 ‰. Balistrieri and others (this volume) extended the Truesdell and others (1977) modeling to sublacustrine vents and associated pore waters in Yellowstone Lake, at Mary Bay. Their studies indicated that the deep reservoir probably underlies the entire caldera and that the prevalence of steam in the eastern caldera is due more to altitude effects than to a fundamental difference in the geothermal systems.

Table 1. δD of drill-hole, hot-spring, and cold-water samples from Yellowstone National Park geyser basins.

Basin	Drill holes	Hot springs	Cold waters
Norris	–149 to –151	–139 to –149	–140 to –144
Lower	–146 to –149	–140 to –146	–140 to –145
Shoshone		–135 to –139	–130 to –135

A single, deep-source water for Yellowstone surface-thermal-water discharges also is indicated by chemical arguments. When chloride compositions and geothermometer temperatures of the thermal waters are plotted on enthalpy-chloride diagrams (fig. 3), the temperatures and chloride concentrations of all major thermal waters in the Park are consistent with derivation from a single deep fluid of 320 ppm chloride and 360°C temperature (Truesdell and Fournier, 1976). Research wells do not exist for West Thumb and Heart Lake Geyser Basins, and mixing of partially evaporated water from Yellowstone and Heart Lakes complicates the δD values of their thermal waters. However, as shown in figure 4, the $\delta^{18}O$ versus chloride systematics of some Heart Lake and West Thumb hot springs are similar to those of waters from Norris, Upper, Lower, and Shoshone Geyser Basins. The fact that the compositions of some thermal waters at Heart Lake and West Thumb fall on the same mixing line as other spring waters suggests that they possibly evolved from the same deep water. All of our data from Yellowstone are consistent with the hypothesis that an isotopically and chemically homogeneous fluid underlies all of the thermal areas on the west side of the caldera.

Methodology for Tracing Recharge Sources

Use of δD in Hydrology Studies of Geothermal Areas

Hydrogen- and oxygen-isotopic compositions of water show variations related to the source and history of the water. For most cold-water systems, these isotopes may be used interchangeably because processes of evaporation and condensation affect both isotopes similarly. For geothermal systems, both isotopes are affected by subsurface processes of mixing, boiling, and steam separation, as discussed and modeled in our earlier paper emphasizing thermal waters (Truesdell and others, 1977). In geothermal systems such as Yellowstone, however, oxygen isotopes in water exchange with those in rock so that $\delta^{18}O$ values of water depend on the temperature and duration of rock-water interaction, on the ratio of water to rock, and on the character of the rock, as well as on mixing and evaporation-condensation processes. This exchange, called the “oxygen isotope shift,” complicates interpretation of the $\delta^{18}O$ values as indicators of recharge. In contrast, hydrogen-isotope exchange between water and rock minerals is not significant (except at very low water/rock ratios), and interpretation

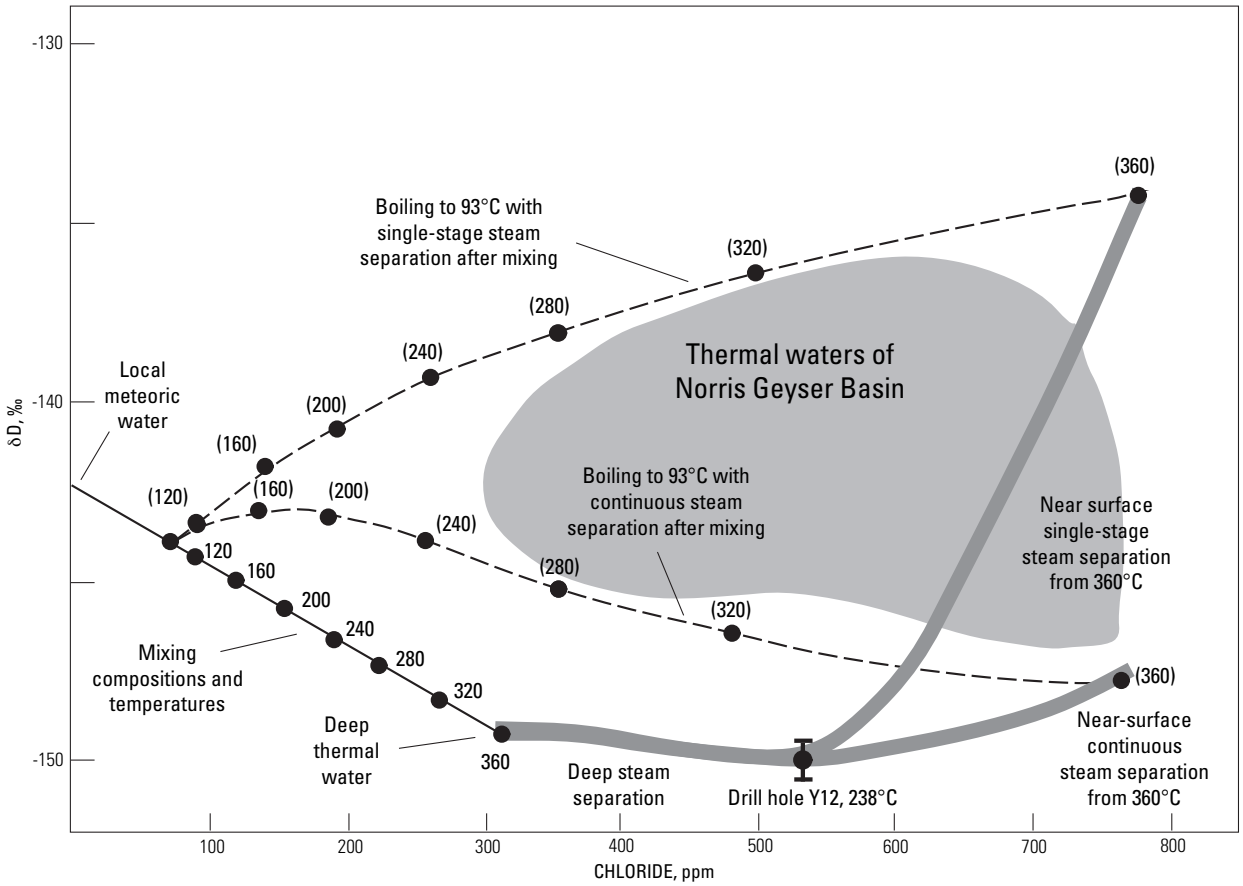

Figure 2. Generalized mixing and boiling model for Norris Geyser Basin waters (from Truesdell and others, 1977). Solid straight line shows compositions and temperatures for mixtures of deep thermal water and surface water. Wide dark-gray lines shows evolved composition of deep waters that undergo single-stage or continuous steam separation from 360° to 93 °C without mixing. Dashed lines show compositions at 93°C for mixed waters after undergoing single-stage or continuous steam separation from mixtures having the indicated starting temperatures (shown in parentheses). Gray field shows compositions of Norris Geyser Basin neutral-chloride hot-spring waters. Similar diagrams using the same deep-water compositions can explain the compositions of hot springs at Upper, Lower, and Shoshone Geyser Basins (Truesdell and others, 1977).

of δD values of water is more straightforward. For this reason, we concentrated our study of Yellowstone recharge on the δD values of possible infiltrating waters in relation to the δD values of the thermal-source water described earlier.

Determination of the recharge area for the deep thermal water requires samples that are representative of infiltrating waters. As is discussed later, possible infiltrating waters are best sampled during dry periods in the fall when most streams and rivers in Yellowstone National Park are fed largely by springs and seeps (the springs and seeps received most of their recharge from snowmelt during the previous spring). More than 300 δD analyses were made of possible infiltrating waters from cold springs, wells, streams, and rivers in a 15,000 km^2 region in and adjacent to the Park. Most of the samples were collected in the fall from 1967 to 1990. The remainder of this section focuses on validating the use of δD analyses of these samples as an indicator of the composition of infiltrating waters. To aid in this validation, $\delta^{18}O$ analyses also were made on some of these samples.

Climatic Controls on the Regional Distribution of the δD of Cold Waters in the Yellowstone Area

A recent study of more than 4,800 δD values of surface waters in the conterminous United States shows the mountainous Yellowstone Plateau to be within a large area with δD values lower than –130 ‰, in which δD contours closely match topographic contours (Kendall and Coplen, 1991, 2001). Yellowstone Park is in a part of North America that is affected by Arctic, Gulf of Mexico, and Pacific air masses (Bryson and Hare, 1974). The general distribution of δD values of cold waters in the Park area reflects the influence of both complex weather patterns and altitude.

Precipitation records in Yellowstone Park were summarized by Dirks and Martner (1982). River runoff records were summarized by Norton and Friedman (1991), and weather patterns were interpreted by Despain (1987). According to precipitation

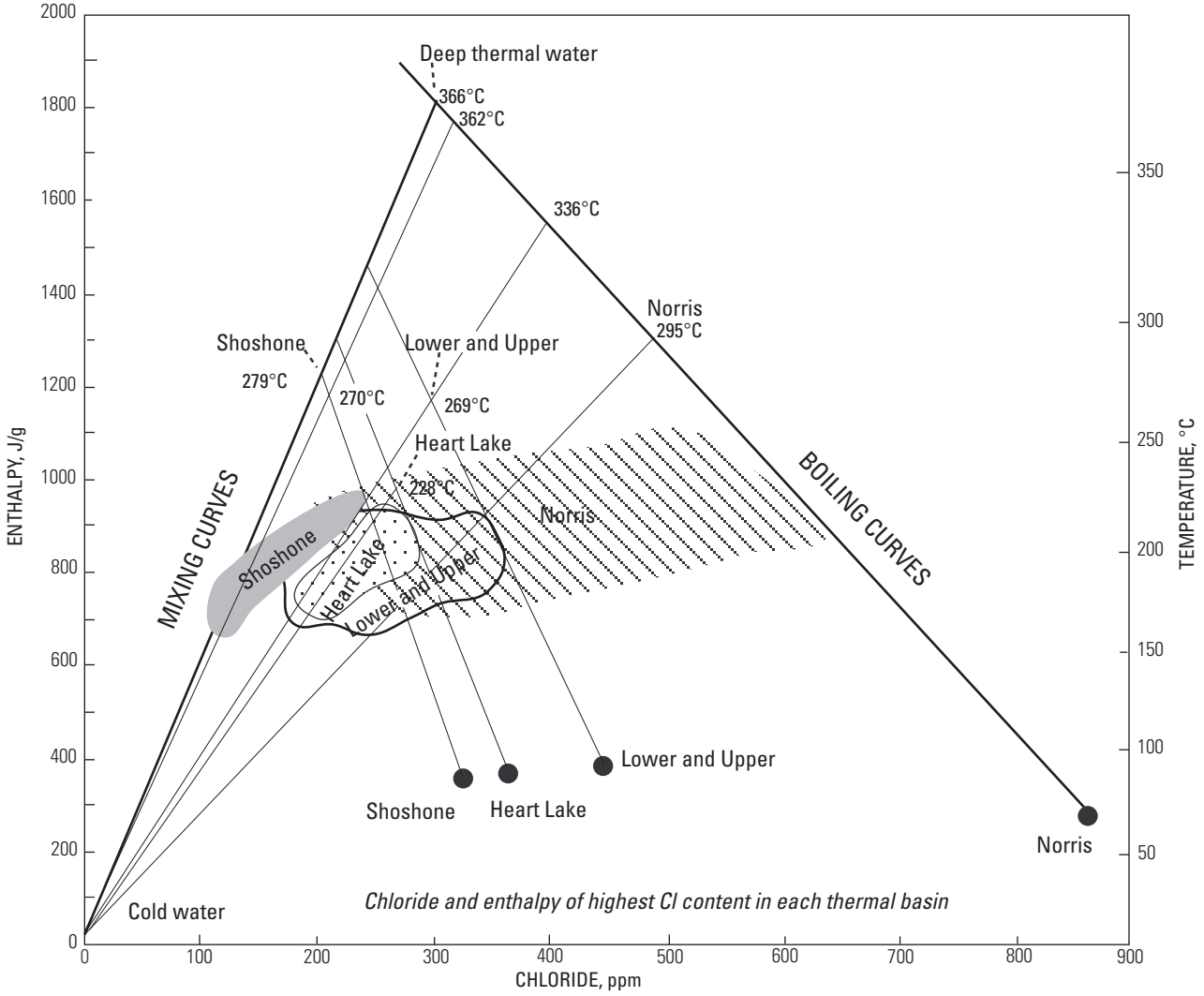

Figure 3. Enthalpy-chloride diagram for Lower, Upper, Norris, Heart Lake, and Shoshone Geyser Basins (from Truesdell and Fournier, 1976). Pattern areas outline compositions for hot neutral-chloride waters in respective geyser basins. Because little heat is lost by conduction and chloride is conservative, all enthalpy and chloride compositions must be a result of mixing and boiling. Diagram shows that all compositions for all basins can be explained as a result of mixing and boiling combinations of a single deep-thermal water having about 320 ppm chloride at 360°C and dilute cold waters.

summaries by Dirks and Martner (1982), precipitation in the region is fairly well distributed throughout the year, with the exception that large storms occur in mid-winter and dry periods frequently occur in the fall. As much as 75 percent of the total precipitation in Yellowstone Park falls during winter snowstorms from October through May. The remainder falls primarily during local warm-season thunderstorms. Because the valleys in the Park tend to be dry, seasonal river-flow measurements for the major drainage basins, such as the Madison River, indicate that most of the precipitation is concentrated at higher altitudes and that it accumulates there as snow, causing high river volumes during spring snowmelt. The largest amount of precipitation falls on the high plateaus in the southwestern part of the Park; the Central Plateau is in the rain shadow of the higher areas to the southwest (Dirks and Martner, 1982; Norton and Friedman, 1991; Farnes, 1997).

The largest storms, from the Pacific, enter the Park region from the Snake River Plain to the southwest. Winter weather in Yellowstone reflects the relative strengths and positions of Arctic and Pacific air masses. The increase in δD values in all directions away from the mountainous Yellowstone Plateau reflects the influence of high altitudes and the complex weather patterns in the region involving Pacific, Arctic, and Gulf air masses. The northward decrease in δD values, shown in our data in a succeeding section, reflects both increases in altitude and the general south-to-north path of storm trajectories, as well as the rain shadow produced by the southwestern mountains. The trend to less negative δD values for cold water in the northeastern part of mountainous regions possibly reflects the importance of Gulf air masses in the eastern part of the region.

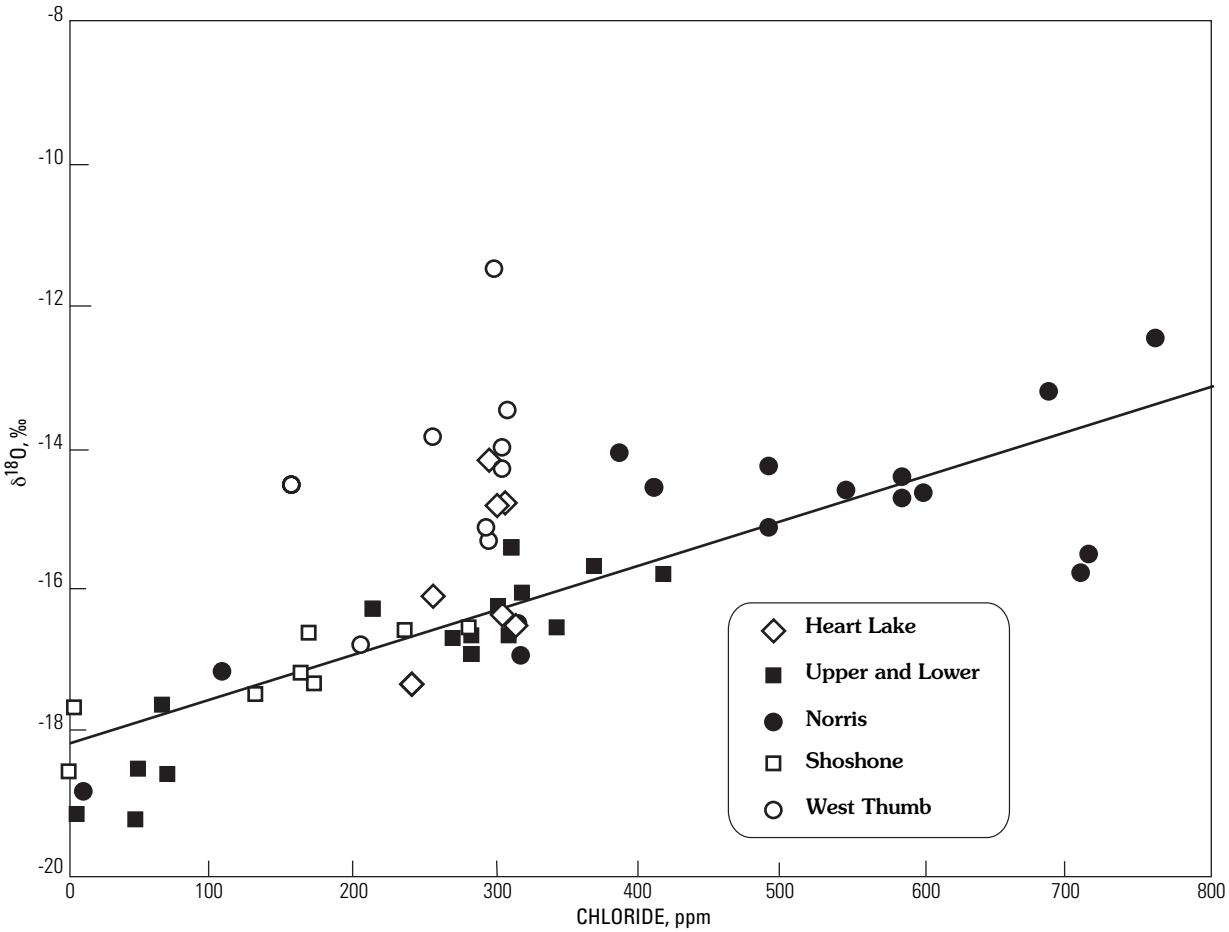

Figure 4. $\delta^{18}O$-chloride relations for neutral-chloride hot-spring waters from the Heart Lake, Upper, Lower, Norris, Shoshone, and West Thumb Geyser Basins. The less negative $\delta^{18}O$ values for hot waters and Heart Lake and West Thumb reflect the mixing of evaporated waters from Heart and Yellowstone Lakes, respectively. The compositions of all hot waters fall on a trend, suggesting the possibility that they evolved from the same deep thermal water. Different isotopic compositions of hot waters in different basins reflect, in large part, mixing of the deep thermal water with local shallow water of different compositions.

$\delta^{18}O$ and δD Values of Precipitation and Cold Waters in Yellowstone National Park

The δD and $\delta^{18}O$ values for precipitation samples collected in the Yellowstone National Park region during May and June and during November and December, 1970 through 1977, are given in table 2. These data and values of cold-water samples from streams, rivers, cold springs, and lakes collected in May and June and in September and October, 1967 through 1982 (table 2), are plotted in figure 5. The data for the precipitation samples plot very close to the global meteoric water line (GMWL) (Craig, 1961) with δD values from –64 to –168 ‰. These data establish that the local meteoric water line (LMWL) in the Yellowstone region is identical within error to the GMWL. Similar results were obtained by Thordsen and others (1992) from snow core samples.

The δD and $\delta^{18}O$ values of the stream, river, and spring samples straddle the GMWL, with δD values from –126 to –153 ‰. These samples are typical of those analyzed only for δD. The conformity of their compositions to the GMWL indicates that our surface-water samples did not undergo significant evaporation during precipitation, infiltration, or inflow into streams. The δD-$\delta^{18}O$ values of lake samples, however, in a fashion typical of evaporated waters, plot off the GMWL. Our data from streams, rivers, and springs contrast with those of Thordsen and others (1992). Their data for springs show increased isotope spreads for higher $\delta^{18}O$ values typical of evaporation trends. Many of their samples show values similar to values we observed for lakes (figure 5) or for streams flowing from lakes. Their study differed from ours in that it included many samples from low-altitude springs and seeps collected during summer months. Water from seeps and small springs is likely to undergo evaporation in the summer. Summer rainfall in the low-altitude valleys of Yellowstone Park, which recharges the seeps and small springs, also is likely to undergo evaporation during precipitation. Such waters will not have compositions typical of infiltrating waters that are derived from melting snow in the spring.

Table 2. δD of precipitation in Yellowstone National Park.

Date sampled	Collection	Amount (cm)	δD (‰)
	Mammoth		
5/30/77	May 1977		–118
1/26/78	Jan. 1978	1.9	–152
10/23/78	June 1978 to Oct. 1978		–90
1/12/79	Jan. 12, 1979	0.8	–206
3/7/79	Mar. 1–7, 1979	6.1	–184
7/30/79	July 1979	3.3	–94
8/31/79	Aug. 1979	5.2	–73
10/15/79	Oct. 15, 1979	1.3	–83
11/12/78	Oct.1 to Nov. 12, 1979		–163
	Old Faithful		
8/31/78	Aug. 1978		–61
10/31/78	Oct. 1978	1.0	–115
3/4/79	Feb. 1979	6.5	–189
3/31/79	Mar. 1979	6.3	–167
5/1/79	Apr. 1979	4.1	–160
5/1/79	Apr. 1979	4.1	–161
5/31/79	May 1979	3.1	–154
6/31/79	June 1979	3.3	–120
7/31/79	July 1979	1.3	–103
8/30/79	Aug. 1979	5.8	–79
9/30/79	Sep. 1979	1.5	–68
11/2/79	Oct. 1979	5.6	–142
12/2/79	Nov. 1979	1.7	–171
1/2/80	Dec. 1979	2.4	–153
1/31/80	Jan. 1980	7.8	–151
3/2/80	Feb. 1980	5.2	–135
4/3/80	Mar. 1980	1.7	–151
5/1/80	Apr. 1980	2.5	–122
6/1/80	May 1980	11.2	–120
7/1/80	June 1980	3.2	–112
8/1/80	July 1980	8.5	–102
9/4/80	Aug. 1980	4.7	–85
11/4/80	Oct. 1980	5.6	–93
12/4/80	Nov. 1980	1.7	–114
1/1/81	Dec. 1980	8.0	–156
7/30/82	July 1982	5.6	–124
9/1/82	Aug. 1982		–113
10/1/82	Sep. 1982	3.3	–186
11/30/92	Nov. 1982	6.9	–143
12/31/82	Dec. 1982	7.7	–188
1/31/83	Jan. 1983	3.1	–138

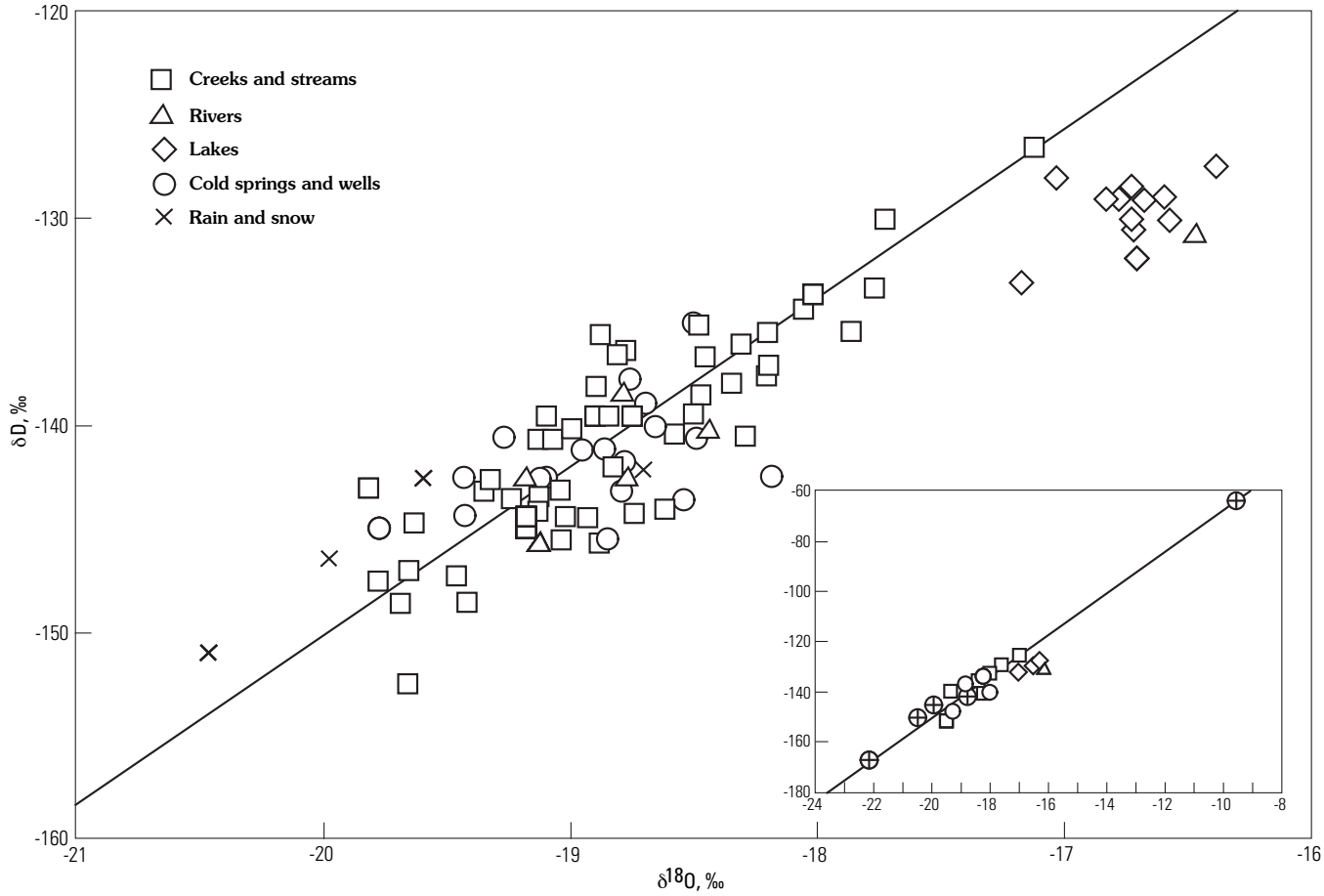

Figure 5. δD-δ^{18}O of precipitation, creeks, streams, rivers, lakes, cold springs, wells, rain, and snow from Yellowstone National Park region showing relationship to Craig's (1961) global meteoric water line. Insert shows same data set with two additional precipitation samples with extreme compositions.

δD of Precipitation in Yellowstone National Park and Its Relationship to δD of Infiltrating Water

Precipitation in a given drainage area can have a wide range of δD values, depending on the temperature, source, and history of air masses responsible for individual storms. Samples collected monthly by Park rangers from rain and snow gages at Mammoth and Old Faithful, from May 1977 through January 1983, allowed us to study the variation of δD of precipitation at those locations during a period of several years. The δD values of the precipitation, along with amounts of precipitation for the collection periods, are summarized in table 3. The δD values ranged from –206 ‰ for a single storm of 0.8 cm of precipitation at Mammoth on January 12, 1979, to –68 ‰ for 1.5 cm of precipitation during September 1979. The δD values of precipitation at Mammoth are similar to those at Old Faithful for the few months that collections were made at both sites. The data for Old Faithful, where precipitation samples were available for nearly every month during a 2-year period, are plotted in figure 6. The δD values of the monthly precipitation collections at Old Faithful show cyclic seasonal variations, in which the most negative values are derived from samples collected during the winter and the least negative values are derived from samples collected during the summer.

The weighted average δD for precipitation during winter months (September–May) of –134 ‰ (table 3) is close to the average value observed for the water supply at Old Faithful (table 4 and next section). Thus, it is likely that ground waters receive most of their recharge from melting snow during spring runoff. Because precipitation in a given drainage area can have a wide range of δD values, determination of the δD of the recharge for the thermal water involves locating cold waters that have the δD value of average infiltrating waters.

In 1967, we assumed that water from wells and cold springs that have steady discharge from ground-water reservoirs, in which water has a relatively long residence time, should give the best average values for water available for recharge. Unfortunately, there are very few such cold springs in the geyser basins where most of the subsurface water at low altitudes is thermal. Collection from cold springs outside the geyser basins is difficult because the springs seldom are located on maps, and they are likely to be small and ephemeral so that the δD of discharging water possibly reflects the most recent

Table 3. δD and $\delta^{18}O$ of streams, rivers, springs, lakes, and precipitation in Yellowstone National Park.

Sample	Description	Date sampled (mo/day/yr)	Temperature (°C)	$\delta^{18}O$ (‰)	δD (‰)
		Streams			
R-25	Tributary of Solfatara Creek	09/10/67	38	–18.6	–144
W-3	Glen Creek	09/21/71		–19.7	–149
W-4	Nez Perce Creek	09/24/71		–19.2	–144
W-13	Glen Creek	10/11/71	7	–19.8	–148
W-18	DeLacy Creek	10/11/71	7	–18.5	–138
W-25	Unnamed creek 2 mi north of Lake	10/12/71	7	–19.7	–145
W-33	Nez Perce Creek	10/04/72	13	–18.8	–144
W-2	Little Creek	10/10/75		–18.8	–136
W-3	Arnica Creek	10/10/75		–19.3	–144
W-4	Cub Creek	10/10/75		–18.9	–135
W-5	Antelope Creek	10/10/75		–19.7	–148
W-6	Tower Creek	10/10/75		–19.4	–143
W-7	Crystal Creek	10/10/75		–18.8	–142
T73-87	Fall Creek	09/10/73		–17.7	–130
T76-14	Creek near Gibbon River	09/10/76	5	–19.4	–142
T76-15	Creek near Dunraven picnic area	09/10/76	5	–19.1	–140
T76-16	Antelope Creek	09/10/76	6	–19.7	–147
T76-17	Tributary of Soda Butte Creek	09/10/76	6	–17.1	–126
T76-18	Soda Butte Creek	09/10/76	6	–18.7	–140
T76-19	Amphitheater Creek	09/10/76	5	–18.6	–141
T76-20	Pebble Creek	09/10/76	5	–19.2	–141
T76-??	DeLacy Creek	09/10/76		–18.4	–138
T76-28	Tributary of Clear Creek	09/10/76		–18.9	–138
T76-29	Cub Creek	09/10/76		–18.8	–136
T76-40	Glen Creek	09/30/76	8	–19.7	–153
T76-43	Tributary to Grayling Creek	09/30/76		–18.6	–140
T76-44	Tributary to Grayling Creek	09/30/76		–19.8	–143
T76-45	Tributary to Grayling Creek	09/30/76		–19.5	–148
T76-46	Tributary to Grayling Creek	09/30/76		–19.5	–147
T76-47	Grayling Creek	09/30/76		–18.6	–140
W-1002	Delacy Creek	06/14/77		–18.1	–134
W-1003	Grayling Creek	06/14/77		–17.8	–133
W-1004	Cub Creek	06/14/77		–19.1	–146
W-1008	Tributary of Grayling Creek	06/14/77		–18.2	–136
W-1009	Pebble Creek	06/14/77		–19.0	–144
W-1010	Glen Creek	06/14/77		–18.2	–138
W-1012	Creek near Virginia Meadows	06/14/77		–18.3	–141
W-1013	Antelope Creek	06/14/77		–19.0	–140
W-1014	Tributary of Barronette Creek	06/14/77		–17.9	–135
W-1015	Dunraven Peak Creek	06/14/77		–18.9	–146
W-1017	Tributary of Clear Creek	06/14/77		–19.1	–143
W-1018	Black Butte Creek	06/14/77		–19.1	–145
W-1019	Tributary of Grayling Creek	06/14/77		–18.2	–137
W-1020	Soda Butte Creek	06/14/77		–19.2	–144
H78-1	Grayling Creek	05/09/78	3	–18.5	–136
H78-2	Grayling Creek	05/09/78	4	–18.5	–135
H78-5	Black Butte Creek	05/09/78	6	–19.2	–145
H78-7	Cub Creek	05/10/78	2	–19.1	–141
H78-10	Glen Creek	05/10/78	4	–19.2	–144
H78-11	Apollinaris Creek	05/10/78	8	–18.5	–141
H78-13	Creek north of Soda Butte	05/11/78	1	–18.5	–140
H78-14	Soda Butte Creek	05/11/78	3	–18.9	–140
H78-15	Pebble Creek	05/11/78	3	–18.9	–140

Table 3. δD and $\delta^{18}O$ of streams, rivers, springs, lakes, and precipitation in Yellowstone National Park—*Continued*.

Sample	Description	Date sampled (mo/day/yr)	Temperature (°C)	$\delta^{18}O$ (‰)	δD (‰)
		Streams—*Continued*			
SH86-11	Shoshone Creek	09/10/86		–18.3	–136
SH86-12	Shoshone Creek	09/10/86		–18.0	–134
		Rivers			
R-41	Gibbon above Virgina Cascades	09/10/67		–18.5	–140
W-2	Gibbon above Virgina Cascades	09/21/71		–18.8	–142
W-12	Gardiner River	10/11/71	8	–19.2	–146
W-17	Little Firehole River	10/11/71	14	–18.8	–138
W-43	Yellowstone River	10/04/72	10	–16.5	–131
W-8	Lamar River	10/10/75		–19.2	–143
T76-13a	Gibbon River	09/10/76		–18.6	–141
		Lakes			
T75-23	Yellowstone Lake, Fishing Bridge	10/06/75		–16.7	–132
T75-24	Yellowstone Lake, Pumice Point	10/06/75		–16.7	–132
T76-30	Yellowstone Lake, Steamboat Point	10/08/75		–16.6	–130
T76-31	Yellowstone Lake, Fishing Bridge	10/08/75		–16.7	–131
T76-32	Yellowstone Lake, Pumice Point	10/08/75		–16.7	–130
W-1005	Yellowstone Lake, Pumice Point	06/14/77		–16.7	–129
W-1006	Yellowstone Lake, Steamboat Point	06/14/77		–17.0	–128
W-1011	Yellowstone Lake, Fishing Bridge	06/14/77		–16.8	–129
W-1016	Yellowstone Lake, Fishing Bridge	06/14/77		–16.8	–129
H78-6	Yellowstone Lake, Pumice Point	05/10/78		–16.7	–129
H78-8	Yellowstone Lake, Steamboat Point	05/10/78		–16.6	–129
H78-9	Yellowstone Lake, Fishing Bridge	05/10/78		–17.2	–133
T81-20	Shoshone Lake	09/19/81		–16.4	–128
		Springs			
F-381	Midway picnic area spring	10/19/67		–18.9	–145
W-1	Midway picnic area water supply	09/29/71		–19.2	–142
W-6	Midway picnic area spring	09/29/71		–19.0	–141
W-9	Above Black Sand Basin	10/10/71		–19.1	–142
W-10	New Old Faithful	10/10/71		–18.8	–138
W-11	Apollinaris	10/10/71		–18.9	–141
F-571	West of Sylvan Springs	09/10/72		–19.3	–140
T73-20	Grants Pass	09/07/73		–18.5	–135
T74-49	Apollinaris	08/10/74		–18.8	–143
T74-59	Apollinaris	10/10/74		–18.8	–143
T75-73	Apollinaris	10/10/74		–18.2	–142
T76-37	Grants Pass	09/10/76		–18.7	–139
W-1007	Apollinaris	06/14/77		–18.6	–140
W-1022	Cold spring	06/14/77		–19.4	–142
H78-3	Near tributary of Grayling Creek	05/09/78		–19.8	–145
H78-4	Cold spring east of culvert	05/09/78		–19.4	–144
H78-11	Apollinaris	05/10/78		–18.5	–141
T82-5	West of Emerald pool	10/01/82		–18.8	–142
T82-19	Apollinaris	10/04/82		–18.6	–144
		Precipitation			
F-486	Near Gibbon	05/27/70		–18.7	–142
T75-87	Mammoth	12/10/75		–22.4	–168
T75-85	Mammoth	11/10/75		–20.0	–146

Table 3. δD and $\delta^{18}O$ of streams, rivers, springs, lakes, and precipitation in Yellowstone National Park—*Continued*.

Sample	Description	Date sampled (mo/day/yr)	Temperature (°C)	$\delta^{18}O$ (‰)	δD (‰)
		Precipitation—*Continued*			
T75-86	Old Faithful	12/10/75		–20.5	–151
T75-84	Old Faithful	11/10/75		–19.6	–142
W-1021	Old Faithful	06/14/77		–9.4	–64

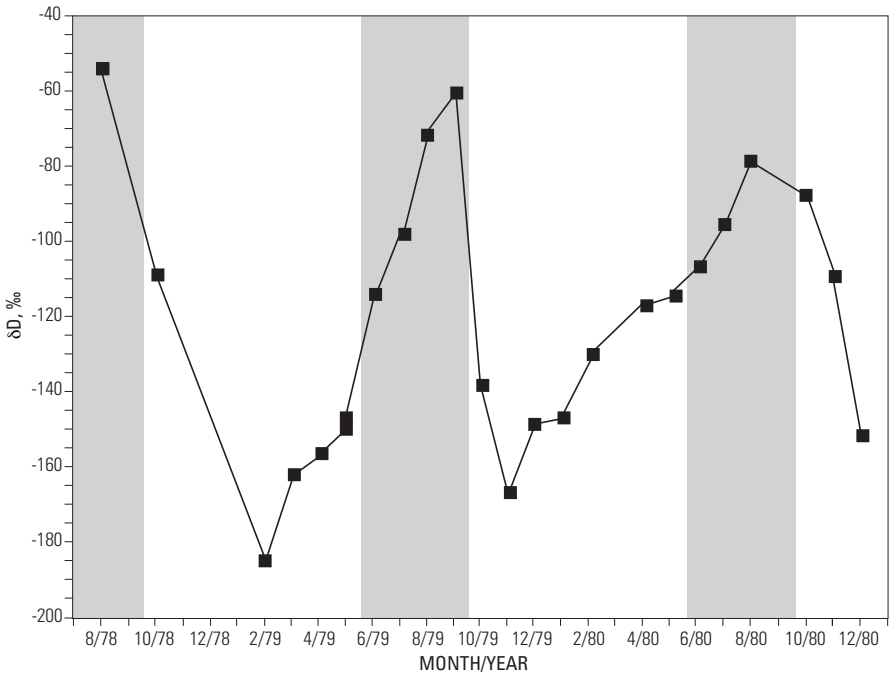

Figure 6. δD of monthly precipitation collections from rain gages at Old Faithful from August 1978 through January 1981.

precipitation rather than a long-term average value. Much of the drinking water in the Park is not from wells but from surface water in reservoirs where evaporation is likely. Because relatively few cold springs and wells were accessible, most of our samples collected after 1967 were from fast-moving cold streams and rivers.

Relationship of δD of Ground Waters to δD of Streams and Rivers

Because sampling of Yellowstone streams was largely limited to the fall season, the isotope systematics of individual streams throughout the year and the relationship of δD values of stream samples to average values for ground water must be predicted by analogy from studies of small cold streams that have been sampled frequently over a period of several years (principles reviewed by Fritz, 1981). In alpine basins with small ground-water-storage capacity, the inflow of ground water causes small sinusoidal annual changes of about ±5 ‰ in δD, with summer values isotopically heavy and winter values light (Hermann and others, 1978). Only the δD of streams during the dry period at the end of summer showed the composition of ground water with a value near that of the average for winter precipitation. Such studies suggest that stream samples collected in the early fall, after the end of summer thunderstorms and before the start of winter storms, probably are representative of ground waters that were recharged largely during the previous spring. Supporting this assumption is an observation that in the Yellowstone region δD values of streams in the fall are mostly within ±4 ‰ of the value recorded for the previous spring (table 4). We do not expect perfect agreement between the values for the spring runoff and fall stream discharge because the ground-water-storage capacity of the reservoirs for springs that feed individual streams probably varies considerably, and some spring reservoirs possibly retain water from several previous years.

Sampling of Streams for δD Analyses

Ideally, the water in streams and rivers should undergo little isotopic change during flow; it should closely reflect the average δD for local ground water feeding the streams through springs and seeps. Ideal streams are those that are fed exclusively from large subsurface reservoirs in which water has a relatively long residence time and has flowed

Table 4. δD of cold waters in Yellowstone National Park and adjacent areas.

Sample	Name	Elevation (meters)	Latitude (N.)	Longitude (W.)	Date (mo/day/yr)	Location	Temperature (°C)	δD (‰)
				GALLATIN RANGE—northwest of Yellowstone National Park				
MH78-21	Spanish Creek	1,620	45°29'	111°16'	10/1/78	before Gallatin River along US 191		-136
MH78-22	Squaw Creek	1,650	45°26'	111°14'	10/1/78	before Gallatin River along US 191		-145
MH78-23	Portal Creek	1,670	45°19'	111°11'	10/1/78	before Gallatin River along US 191		-142
MH78-2	Dudley Creek	1,830	45°15'	111°14'	9/7/78	before Gallatin River along US 191	9	-147
MH78-3	Dudley Creek Spring	1,830	45°15'	111°14'	9/7/78	north of Dudley Creek	14	-149
MH78-4	Porcupine Creek	1,860	45°13'	111°15'	9/7/78	before Gallatin River along US 191	13	-147
MH78-5	Beaver Creek	1,860	45°13'	111°11'	9/7/78	before Gallatin River along US 191		-145
MH78-6	Buck Creek	1,920	45°10'	111°15'	9/7/78	before Gallatin River along US 191		-147
MH78-7	Elkhorn Creek	1,920	45°09'	111°15'	9/7/78	before Gallatin River along US 191	7.5	-148
MH78-1	Buffalo Horn Creek	1,950	45°06'	111°13'	9/6/78	before Gallatin River along US 191	15	-144
MH78-8	Taylor Fork	2,040	45°04'	111°16'	9/7/78	before Wapati Creek	15	-138
MH78-9	Wapiti Creek	2,040	45°04'	111°16'	9/7/78	north of Taylor Creek	15	-139
MH78-10	Taylor Fork Spring	2,010	45°04'	111°10'	9/8/78	at rockpile near Taylor Fork	17	-135
MH78-11	Sage Creek	2,010	45°04'	111°11'	9/7/78	before Big Spring Creek	15	-137
MH78-12	Snowflake Spring	2,010	45°04'	111°11'	9/9/78	1/4 mile south of US 191	12	-152
				ABSAROKA-BEARTOOTH RANGE—*WEST*				
R78-28	Pine Creek		45°30'	110°21'	10/2/78	at quarry 3 mile east of US 89		-141
R78-29	Mill Creek	1,980	45°16'	110°29'	10/2/78	1/2 mile east of Anderson Creek		-143
R78-30	Montanapolis Spring	1,800	45°17'	110°31'	10/2/78	north of Mill Creek Ranch		-152
R78-31	West Fork Mill Creek tributary	1,980	46°14'	110°34'	10/2/78	1/2 mile south Coffee Pot Creek		-147
R78-32	West Mill Creek	1,860	45°16'	110°35'	10/2/78	before Arrastra Creek		-144
R78-33	Arrastra Creek	2,100	45°16'	110°36'	10/2/78	at road to Barbara Ann mine		-148
R78-34	East Fork Mill Creek	1,740	45°19'	110°31'	10/2/78	at Snowy Range Ranch		-148
R78-35	Emigrant Creek	1,830	45°18'	110°41'	10/2/78	end of road in Emigrant Gulch		-142
R78-36	Six Mile Creek	1,620	45°17'	110°46'	10/2/78	at fork in road to Dailey Lake		-144
R78-37	Cedar Creek	1,740	45°09'	110°47'	10/2/78	at road crossing west of ranch		-145
R78-38	Pine Creek	2,100	45°05'	110°37'	10/2/78	at road crossing north of Jardine		-145
R78-39	North Fork Bear Creek	2,120	45°05'	110°38'	10/2/78	at Bear Creek Trail west of Jardine		-149
R78-40	Bear Creek	1,980	45°05'	110°38'	10/2/78	at Jardine		-146
				ABSAROKA-BEARTOOTH RANGE—*CENTRAL*				
R78-19	Stillwater River	1,560	45°21'	109°54'	9/30/78	at campground .5 mile west Beartooth Ranch		-138
R78-20	Woodbine Creek	1,560	45°21'	109°53'	9/30/78	below falls trail before Stillwater River		-137
R78-21	Stillwater River	1,100	45°39'	109°18'	9/30/78	before Yellowstone River near Columbus		-138
R78-22	Boulder River	2,040	45°16'	110°15'	10/1/78	at Box Canyon Guard Station		-148
R78-23	Four Mile Creek	1,860	45°20'	110°14'	10/1/78	before Boulder River		-147
R78-24	Speculator Creek	1,710	45°23'	110°12'	10/1/78	before Boulder River		-147

Table 4. δD of cold waters in Yellowstone National Park and adjacent areas—*Continued*.

Sample	Name	Elevation (meters)	Latitude (N.)	Longitude (W.)	Date (mo/day/yr)	Location	Temperature (°C)	δD (‰)
				ABSAROKA-BEARTOOTH RANGE—*CENTRAL—Continued*				
R78-25	East Chippy Creek	1,680	45°26'	110°11'	10/1/78	before Boulder River (near Weasel Creek)		-146
R78-26	Boulder River	1,460	45°40'	110°06'	10/1/78	before east Boulder River on State 298		-144
R78-27	West Boulder River	1,490	45°37'	110°15'	10/1/78	before Boulder River on road to Livingston		-145
				ABSAROKA-BEARTOOTH RANGE—*EAST*				
R78-12	Cook City Creek	2,350	45°01'	109°55'	9/29/78	on east side of Cooke City on US 212		-139
R78-13	Clarks Fork River	2,130	44°57'	109°48'	9/29/78	below Pilot Creek at US 212 bridge		-136
R78-14	Rock Creek	2,130	45°04'	109°24'	9/29/78	before Lake Fork on US 212		-140
R78-15	W. Fork Rock Creek	2,350	45°10'	109°29'	9/29/78	at Camp Senia		-141
R78-16	East Rosebud Creek	1,890	45°12'	109°39'	9/30/78	at outlet from east Rosebud Lake		-138
R78-17	East Rosebud Creek spring	1,770	45°13'	109°38'	9/30/78	north side east Rosebud 1 mile east of lake		-145
R78-18	West Rosebud Creek	1,370	45°27'	109°30'	9/30/78	before Fishtail Creek at Highway near Fishtail		-139
				GALLATIN RANGE YNP				
W-12	Gardiner River	2,260	44°54'	110°45'	10/11/71	at US 89 near Indian Creek campground		-146
R82-31	Gardiner River	2,260	44°54'	110°45'	9/22/82	at US 89 near Indian Creek campground	5.5	-145
R82-32	Gardiner River	2,260	44°54'	110°45'	9/28/82	at service road before Panther-Indian Creeks	5	-147
R78-6	Gardiner River	2,260	44°54'	110°45'	9/29/78	at bridge on Grand Loop Road		-140
R90-35	Gardiner River	2,260	44°54'	110°45'	9/12/90	at Fawn Pass trail crossing	15	-142
F-478	Glen Creek	2,230	44°56'	110°44'	5/25/70	north of Rustic Falls on US 89		-147
W-3	Glen Creek	2,230	44°56'	110°44'	9/29/71	north of Rustic Falls on US 89		-149
W-13	Glen Creek	2,230	44°56'	110°44'	10/11/71	north of Rustic Falls on US 89		-148
T76-40	Glen Creek	2,230	44°56'	110°44'	9/30/76	north of Rustic Falls on US 89		-153
W-1010	Glen Creek	2,230	44°56'	110°44'	6/14/77	north of Rustic Falls on US 89		-138
T78-66	Glen Creek	2,230	44°56'	110°44'	9/29/78	north of Rustic Falls on US 89		-153
R79-23	Glen Creek	2,230	44°56'	110°44'	9/24/79	north of Rustic Falls on US 89		-148
R82-33	Glen Creek	2,230	44°56'	110°44'	9/28/82	north of Rustic Falls on US 89 (after storms)	5	-152
R82-14	Glen Creek	2,230	44°56'	110°44'	9/28/82	north of Rustic Falls on US 89	9	-151
R90-25	Glen Creek	2,230	44°56'	110°44'	9/12/90	north of Rustic Falls on US 89 (10:50 AM)	7	-147
R90-37	Glen Creek	2,230	44°56'	110°44'	9/12/90	north of Rustic Falls on US 89 (6:00 PM)	13	-148
R90-26	East Fawn Creek	2,410	44°57'	110°49'	9/12/90	on Fawn Pass trail	12	-141
R90-27	East Fawn Creek spring	2,530	44°57'	110°49'	9/12/90	spring north of Fawn at west end of marshes	7	-147
R90-32	East Fawn Creek spring	2,410	44°57'	110°48'	9/12/90	middle spring south of above	4.5	-147
R90-33	East Fawn Creek spring	2,410	44°57'	110°48'	9/12/90	easternmost spring south of above	5	-146
MH78-14	Indian Creek	2,260	44°53'	110°45'	9/29/78	at Indian Creek campground below Panther Creek		-140
R90-39	Indian Creek	2,260	44°53'	110°45'	9/14/90	trail crossing near Panther Creek (11:00 AM)	9	-138
R90-42	Indian Creek	2,260	44°53'	110°45'	9/14/90	same location (3:00 PM)	13	-138
R90-41	Indian Creek	2,270	44°52'	110°48'	9/14/90	before gravel flats	8	-135

Table 4. δD of cold waters in Yellowstone National Park and adjacent areas—*Continued*.

Sample	Name	Elevation (meters)	Latitude (N.)	Longitude (W.)	Date (mo/day/yr)	Location	Temperature (°C)	δD (‰)
				GALLATIN RANGE YNP—*Continued*				
R90-40	Panther Creek	2,380	44°53'	110°49'	9/14/90	on Bighorn Pass trail	6. 5	-139
R67-2	Apollinaris Spring	2,230	44°51'	110°44'	9/1/67	east of US 89		-144
R82-4	Daly Creek	2,070	45°04'	111°08'	9/22/82	before Gallatin River at US 191	14	-151
R90-10	Daly Creek	2,070	45°04'	111°08'	9/12/90	before Gallatin River at US 191	5	-146
W-807	Black Butte Creek	2,200	45°03'	111°07'	9/30/76	before Gallatin River at US 191		-149
W-1018	Black Butte Creek	2,200	45°03'	111°07'	6/14/77	before Gallatin River at US 191		-145
MH78-15	Black Butte Creek	2,200	45°03'	111°07'	9/30/78	before Gallatin River at US 191		-148
R79-8	Black Butte Creek	2,200	45°03'	111°07'	9/23/79	before Gallatin River at US 191	6	-143
R82- 5	Black Butte Creek	2,200	45°03'	111°07'	9/22/82	before Gallatin River at US 191	9	-151
R90-11	Black Butte Creek	2,200	45°03'	111°07'	9/12/90	before Gallatin River at US 191	4	-146
MH78-16	Specimen Creek	2,200	45°01'	111°05'	9/30/78	before Gallatin River at US 191		-147
R79-7	Specimen Creek	2,200	45°01'	111°05'	9/23/79	before Gallatin River at US 191	6	-144
R82-6	Specimen Creek	2,200	45°01'	111°05'	9/22/82	before Gallatin River at US 191	9	-146
R90-12	Specimen Creek	2,200	45°01'	111°05'	9/12/90	before Gallatin River at US 191	4	-139
R79-6	Fan Creek	2,230	44°57'	111°04'	9/23/79	before Gallatin River at US 191	6	-139
R90-17	Fan Creek	2,230	44°57'	111°04'	9/12/90	before Fawn Creek on Fawn Pass trail	15	-144
R90-13	Fawn Creek trail spring	2,230	44°57'	111°04'	9/12/90	westernmost spring south of Fawn Creek	5.5	-145
R90-15	Fawn Creek trail spring	2,230	44°57'	111°04'	9/12/90	easternmost spring south of Fawn Creek	5.5	-142
R90-16	Fawn Creek trail spring	2,230	44°57'	111°04'	9/12/90	just above Fan Creek on Fawn Pass trail	12	-142
MH78-17	Gallatin River	2,200	44°56'	111°04'	9/30/78	at Bighorn Pass trail head at US 191		-143
R79-9	Gallatin River	2,200	44°56'	111°04'	9/23/79	at Bighorn Pass trail head at US 191	6	-139
T76-47	Grayling Creek	2,160	44°53'	111°03'	9/30/76	before main creek turns S at US 191		-140
W-1003	Grayling Creek	2,160	44°53'	111°03'	6/14/77	before main creek turns S at US 191		-133
MH78-18	Grayling Creek	2,160	44°53'	111°03'	9/30/78	before main creek turns S at US 191		-139
R90-18	Grayling Creek	2,160	44°53'	111°03'	9/12/90	before main creek turns S at US 191	11	-138
R79-5	Grayling Creek	2,160	44°53'	111°03'	9/23/79	before main creek turns S at US 191	6	-135
T76-46	Grayling Creek spring	2,160	44°52'	111°03'	9/30/76	Spring near US 191 between above and below		-147
MH78-24	Grayling Creek spring	2,160	44°52'	111°03'	10/1/78	Spring near US 191 between above and below		-143
R79-4	Grayling Creek spring	2,160	44°52'	111°03'	9/23/79	Spring near US 191 (very little flow)	6	-136
T76-44	Grayling Creek tributary	2,100	44°51'	111°03'	9/30/76	east tributary at State boundary and US 191		-143
W-1019	Grayling Creek tributary	2,100	44°51'	111°04'	6/22/77	east tributary at State boundary and US 191		-137
T76-43	Grayling Creek tributary	2,100	44°51'	111°04'	9/30/76	1 mi southwest of State boundary on US 191		-140
W-1008	Grayling Creek tributary	2,100	44°51'	111°04'	6/14/77	1 mi southwest of State boundary on US 191		-136
R79-3	Grayling Creek tributary	2,100	44°51'	111°04'	9/23/79	1 mi southwest of State boundary on US 191	6.5	-139
R82-7	Grayling Creek tributary	2,100	44°51'	111°04'	9/22/82	1 mi southwest of State boundary on US 191		-145
MH78-19	Duck Creek	2,040	44°47'	111°07'	9/30/78	at US 191		-141
R79-1	Duck Creek	2,040	44°47'	111°07'	9/23/79	at US 191	9.5	-137
R90-19	Duck Creek	2,040	44°47'	111°07'	9/12/90	at US 191	18	-136
MH78-20	Cougar Creek	2,000	44°45'	111°07'	9/30/78	at US 191		-142

Table 4. δD of cold waters in Yellowstone National Park and adjacent areas—*Continued*.

Sample	Name	Elevation (meters)	Latitude (N.)	Longitude (W.)	Date (mo/day/yr)	Location	Temperature (°C)	δD (‰)
				GALLATIN RANGE YNP—*Continued*				
R79-2	Cougar Creek	2,000	44°45'	111°07'	9/23/79	at US 191	9	-138
R90-21	Pipe Creek	2,180	45°02'	110°52'	9/11/90	tributary to Mol Heron Creek, .5 mi N. of Park	6	-141
R90-24	Reese Creek	1,700	45°03'	110°47'	9/11/90	1.5 mi southwest of US 89	7	-143
				WASHBURN RANGE				
R78-1	Lava Creek	2,070	44°56'	110°38'	9/29/78	before Lupine at Lava Creek Campground		-146
R82-15	Lava Creek	2,070	44°56'	110°38'	9/22/82	before Lupine at Lava Creek Campground	9.5	-148
R82-34	Lava Creek	2,070	44°56'	110°38'	9/28/82	before Lupine at Lava Creek (after storm)	6	-150
R90-3	Lava Creek	2,070	44°56'	110°38'	9/10/90	before Lupine at Lava Creek Campground	15	-146
R90-4	Lupine Creek	2,070	44°56'	110°38'	9/10/90	before Lava Creek	15	-147
R78-2	Blacktail Creek	2,070	44°56'	110°36'	9/29/78	after Deer Creek		-145
R82-16	Blacktail Creek	2,070	44°56'	110°36'	9/22/82	after Deer Creek	11	-144
R82-35	Blacktail Creek	2,070	44°56'	110°36'	9/28/82	after Deer Creek (after storms)	5	-149
R90-5	Blacktail Creek	2,070	44°56'	110°36'	9/10/90	after Deer Creek	16	-145
R90-6	Deer Creek	2,070	44°57'	110°36'	9/10/90	east of Blacktail Creek	14	-141
R78-3	Elk Creek	2,040	44°56'	110°27'	9/29/78	at Grand Loop highway (after storms)		-147
R82-17	Elk Creek	2,040	44°56'	110°27'	9/22/82	at Grand Loop highway	6.5	-147
R90-7	Elk Creek	2,040	44°56'	110°27'	9/10/90	at Grand Loop highway	12	-143
W75-6	Tower Creek	2,040	44°55'	110°25'	11/5/75	above Tower falls		-144
R78-4	Tower Creek	2,040	44°55'	110°25'	9/29/78	above Tower falls		-144
R82-18	Tower Creek	2,040	44°55'	110°25'	9/22/82	above Tower falls	11	-146
R82-41	Tower Creek	2,040	44°55'	110°25'	9/28/82	above Tower falls (after storms)	6	-150
R90-8	Tower Creek	2,040	44°55'	110°25'	9/10/90	above Tower falls	13	-144
W75-5	Antelope Creek	2,130	44°54'	110°23'	11/5/75	at Grand Loop highway		-148
W-785	Antelope Creek	2,130	44°54'	110°23'	9/27/76	at Grand Loop highway		-153
W-1014	Antelope Creek	2,130	44°54'	110°23'	6/14/77	at Grand Loop highway		-147
R78-5	Antelope Creek	2,130	44°54'	110°23'	9/29/78	at Grand Loop highway		-152
R79-10	Antelope Creek	2,130	44°54'	110°23'	9/24/79	at Grand Loop highway		-149
R82-19	Antelope Creek	2,130	44°54'	110°23'	9/22/82	at Grand Loop highway		-150
R90-9	Antelope Creek	2,130	44°54'	110°23'	9/10/90	at Grand Loop highway	13	-147
W-784	Dunraven Peak Creek	2,590	44°46'	110°27'	9/27/76	at Grand Loop highway		-144
W-1015	Dunraven Peak Creek	2,590	44°46'	110°27'	6/14/77	at Grand Loop highway		-146
MH78-13	Dunraven Peak Creek	2,590	44°46'	110°27'	9/29/78	at Grand Loop highway		-143
				BUFFALO PLATEAU				
R77-7	Buffalo Plateau creek	1,950	44°59'	110°26'	10/10/77	at Hellroaring Creek, .5 mi S. State boundary		-150
R77-10	Little Cottonwood Creek	1,770	45°00'	110°29'	10/10/77	at Black Canyon Yellowstone trail		-146
R77-11	Black Canyon trail spring	1,760	45°00'	110°30'	10/10/77	small spg. on Black Canyon Yellowstone trail		-159

Table 4. δD of cold waters in Yellowstone National Park and adjacent areas—*Continued*.

Sample	Name	Elevation (meters)	Latitude (N.)	Longitude (W.)	Date (mo/day/yr)	Location	Temperature (°C)	δD (‰)
				BUFFALO PLATEAU—*Continued*				
R78-11	Slough Creek	1,920	44°57'	110°31'	9/29/78	above Buffalo Creek		-142
R82-24	Slough Creek	1,920	44°57'	110°31'	9/22/82	below Buffalo Creek at campground	12	-142
R82-36	Slough Creek	1,920	44°57'	110°31'	9/28/82	same (after storm)		-146
R90-48	Slough Creek	1,920	44°57'	110°31'	9/12/90	below Buffalo Creek at campground	16	-140
R82-38	Slough Creek campground well	1,920	44°57'	110°31'	9/28/82	well at Buffalo Creek campground		-143
R90-49	Slough Creek campground well	1,920	44°57'	110°31'	9/12/90	well at Buffalo Creek campground	18	-141
R82-37	Buffalo Creek	1,920	44°57'	110°31'	9/28/82	above Slough Creek (after storm)	6	-143
				MADISON PLATEAU				
R78-41	Little Firehole River	2,380	45°29'	110°52'	10/5/78	just above Mystic Falls		-139
R67-1	Little Firehole River	2,380	45°29'	110°52'	9/1/67	just above Mystic Falls		-142
R82-26	Little Firehole River	2,380	45°29'	110°52'	9/23/82	just above Mystic Falls	11	-141
R90-56	Little Firehole River	2,380	45°29'	110°52'	9/15/90	just above Mystic Falls	14	-141
W-9	Black Sand Basin spring	2,320	45°27'	110°52'	10/10/71	base of Rhyolite cliffs above Black Sand basin		-143
R78-42	Black Sand Basin spring	2,320	45°27'	110°52'	10/5/78	base of Rhyolite cliffs above Black Sand basin	4	-139
R82-25	Black Sand Basin spring	2,320	45°27'	110°52'	9/23/82	base of Rhyolite cliffs above Black Sand basin	10	-143
R90-38	Black Sand Basin spring	2,320	45°27'	110°52'	9/13/90	base of Rhyolite cliffs above Black Sand basin	11	-141
W-5	Lonestar road spring	2,320	45°26'	110°48'	9/29/71	by road to Lonestar geyser		-142
R82-27	Madison River	2,040	45°39'	111°01'	9/29/82	at Madison Range overlook	17	-145
R82-42	Madison River	2,040	45°39'	111°01'	9/28/82	at Madison Range overlook	11	-146
R82-72	Boundary Creek	2,040	44°11'	111°00'	9/30/82	1/2 mi before Bechler River on Bechler trail	11	-136
R82-73	Snow Creek	2,040	44°15'	111°06'	10/1/82	at Park boundary road 509	7	-135
R82-74	South Fork Partridge Creek	2,040	44°20'	111°08'	10/1/82	1 mi north of Snow Creek at Park boundary	3	-135
				CENTRAL PLATEAU				
R67-41	Gibbon River	2,380	44°43'	110°39'	9/1/67	just above Virginia Cascades	7	-140
F-486	Gibbon River	2,380	44°43'	110°39'	5/25/70	just above Virginia Cascades		-142
W-2	Gibbon River	2,380	44°43'	110°39'	9/29/71	just above Virginia Cascades		-142
W-782	Gibbon River	2,380	44°43'	110°39'	9/27/76	just above Virginia Cascades		-142
R82-9	Gibbon River	2,380	44°43'	110°39'	9/21/82	just above Virginia Cascades	10	-143
R90-20	Gibbon River	2,380	44°43'	110°39'	9/11/90	just above Virginia Cascades	15	-140
W-783	Gibbon River	2,380	44°43'	110°38'	9/27/76	Virginia Meadows area		-144
W-1012	Gibbon River	2,380	44°43'	110°38'	6/14/77	Virginia Meadows area		-142
MH78-25	Gibbon River	2,380	44°43'	110°38'	10/5/78	Virginia Meadows area		-143
W-27	Gibbon Hill stream	2,320	44°43'	110°41'	10/2/72	small unnamed stream on Gibbon Hill		-141
T78-63	Norris Geyser Basin	2,290	44°44'	110°42'	10/5/78	cold water supply		-140
W-33	Nez Perce Creek	2,200	44°35'	110°47'	10/4/72	at gate to service road		-144
W-4	Nez Perce Creek	2,200	44°35'	110°47'	9/29/71	at gate to service road		-144

Table 4. δD of cold waters in Yellowstone National Park and adjacent areas—*Continued*.

Sample	Name	Elevation (meters)	Latitude (N.)	Longitude (W.)	Date (mo/day/yr)	Location	Temperature (°C)	δD (‰)
				CENTRAL PLATEAU—*Continued*				
R82-29	Nez Perce Creek	2,200	44°35'	110°47'	9/25/82	1 mile east of gate to service road	19	-149
R90-43	Nez Perce Creek	2,200	44°35'	110°47'	9/14/90	100 yds. east of US 89	16.5	-145
W-6	Midway Geyser Basin spring	2,260	44°32'	110°50'	9/29/71	at Lower Basin picnic ground		-141
W75-1	Midway Geyser Basin spring	2,260	44°32'	110°50'	10/10/75	at Lower Basin picnic ground		-142
W-18	Delacy Creek	2,440	44°26'	110°41'	10/11/71	about 100 yards north of US 89		-138
W-792	Delacy Creek	2,440	44°26'	110°41'	9/28/76	about 100 yards north of US 89		-141
W-1002	Delacy Creek	2,440	44°26'	110°41'	6/21/77	about 100 yards north of US 89		-134
MH78-26	Delacy Creek	2,440	44°26'	110°41'	10/5/78	about 100 yards north of US 89		-136
R79-16	Delacy Creek	2,440	44°26'	110°41'	9/24/79	about 100 yards north of US 89		-138
R90-55	Delacy Creek	2,440	44°26'	110°41'	9/15/90	about 100 yards north of US 89	8	-137
R90-54	Dry Creek	2,440	44°26'	110°41'	9/15/90	north of bridge on highway	6	-138
W-10	Old Faithful drinking water	2,240	44°26'	110°48'	10/10/71	cold water supply		-138
MH78-27	Old Faithful drinking water	2,240	44°26'	110°48'	10/5/78	cold water supply		-134
W-25	Lake Junction area creek	2,380	44°35'	110°23'	10/12/71	small creek 2 mi north Lake Junction		-145
R90-44	Lake Junction area creek	2,380	44°35'	110°23'	9/14/90	small creek 2 mi north Lake Junction	9	-140
R82-11	Yellowstone Lake area creek	2,380	44°33'	110°25'	9/21/82	small creek 2 miles north of Yellowstone Lake	10	-148
W-43	Yellowstone River	2,380	44°36'	110°22'	10/4/72	near Cascade campground		-125
R82-10	Yellowstone River	2,380	44°36'	110°22'	9/21/82	near Cascade campground		-130
	Yellowstone River	2,380	44°36'	110°22'	10/5/78	at Fishing bridge		-130
R79-21	Yellowstone River	2,380	44°34'	110°22'	9/24/79	at Fishing bridge		-127
R90-45	Yellowstone Lake	2,380	44°34'	110°22'	9/14/90	at Fishing bridge	20	-128
W75-3	Arnica Creek	2,380	44°28'	110°32'	10/10/75	north of Grand Loop Road		-144
	Arnica Creek	2,380	44°28'	110°32'	10/5/78	north of Grand Loop Road		-148
R79-17	Arnica Creek	2,380	44°28'	110°32'	9/24/79	north of Grand Loop Road		-143
R82-12	Arnica Creek	2,380	44°28'	110°32'	9/21/82	north of Grand Loop Road	14	-146
R90-2	Arnica Creek	2,380	44°28'	110°32'	9/10/90	north of Grand Loop Road	16	-146
W75-2	Little Thumb Creek	2,350	44°25'	110°35'	10/10/75	west of US 89		-137
R79-22	Little Thumb Creek	2,350	44°25'	110°35'	9/24/79	west of US 89		-133
				MIRROR PLATEAU				
R76-13	Specimen Ridge trail spring	2,680	44°49'	110°14'	9/30/76	on Specimen trail		-144
R76-14	Amethyst Creek	2,010	44°53'	110°14'	9/30/76	on Specimen trail		-145
W75-7	Crystal Creek	1,890	44°55'	110°18'	10/5/75	above Lamar River on US 212		-143
R90-52	Crystal Creek	1,890	44°55'	110°18'	9/14/90	above Lamar River on US 212	10	-145
				ABSAROKA RANGE				
R76-5	Lamar River	2,130	44°52'	110°11'	9/30/76	at trail before Lamar River		-142
R76-6	Miller Creek	2,130	44°46'	110°06'	9/30/76	at trail before Lamar River		-143

Table 4. δD of cold waters in Yellowstone National Park and adjacent areas—*Continued*.

Sample	Name	Elevation (meters)	Latitude (N.)	Longitude (W.)	Date (mo/day/yr)	Location	Temperature (°C)	δD (‰)
				ABSAROKA RANGE—*Continued*				
R76-7	Calfee Creek	2,100	44°47'	110°07'	9/30/76	at trail before Lamar River		-142
R76-10	Cache Creek	2,040	44°50'	110°10'	9/30/76	at trail before Miller Creek		-140
W75-8	Larmar River	2,010	44°52'	110°12'	10/5/75	after Soda Butte		-142
R78-7	Larmar River	2,010	44°52'	110°11'	9/29/78	after Soda Butte		-141
R82-23	Larmar River	2,010	44°52'	110°11'	9/22/82	after Soda Butte		-143
R82-40	Larmar River	2,010	44°52'	110°11'	9/28/82	after Soda Butte (very muddy after storm)		-157
R82-21	Larmar River	2,010	44°52'	110°11'	9/22/82	after Soda Butte	7	-142
R90-51	Larmar River	2,010	44°52'	110°11'	9/14/90	after Soda Butte	10	-139
W-789	Pebble Creek	2,070	44°55'	110°07'	9/27/76	at Pebble Creek campground		-146
W-1009	Pebble Creek	2,070	44°55'	110°07'	6/14/77	at Pebble Creek campground		-144
R78-9	Pebble Creek	2,070	44°55'	110°07'	9/29/78	at Pebble Creek campground		-142
R79-13	Pebble Creek	2,070	44°55'	110°07'	9/24/79	at Pebble Creek campground		-143
R82-22	Pebble Creek	2,070	44°55'	110°07'	9/22/82	at Pebble Creek campground	10	-144
R90-50	Pebble Creek	2,070	44°55'	110°07'	9/14/90	at Pebble Creek campground	13	-139
R78-11	Soda Butte Creek	2,200	45°00'	110°00'	9/29/78	at park entrance		-140
W-1020	Soda Butte Creek	2,010	44°55'	110°06'	6/14/77	above Amphitheater		-144
W-787	Soda Butte Creek	2,010	44°52'	110°11'	9/27/76	above Lamar		-142
R82-20	Soda Butte Creek	2,010	44°52'	110°11'	9/22/82	above Lamar		-142
R82-39	Soda Butte Creek	2,010	44°52'	110°11'	9/28/82	above Lamar (after storm)	8	-147
W-788	Amphitheater Creek	2,100	44°55'	110°06'	9/27/76	above Soda Butte		-136
R79-14	Amphitheater Creek	2,100	44°55'	110°06'	9/24/79	above Soda Butte		-142
R82-21	Amphitheater Creek	2,100	44°55'	110°06'	9/22/82	above Soda Butte		-142
W75-4	Cub Creek	2,560	44°30'	110°12'	11/5/75	at US 20		-137
W-1004	Cub Creek	2,560	44°30'	110°12'	6/14/77	at US 20		-146
W-795	Cub Creek	2,560	44°30'	110°12'	9/28/76	at US 20		-142
W-796	Cub Creek	2,560	44°30'	110°12'	10/1/76	at US 20		-142
MH78-30	Cub Creek	2,560	44°30'	110°12'	10/5/78	at US 20		-141
R79-18	Cub Creek	2,560	44°30'	110°12'	9/26/79	at US 20		-137
R90-46	Cub Creek	2,560	44°30'	110°12'	9/14/90	at US 20	16	-139
W-795	Clear Creek	2,560	44°29'	110°10'	10/1/76	at US 20		-142
W-1017	Clear Creek	2,560	44°29'	110°10'	6/14/77	at US 20		-143
R79-20	Clear Creek	2,560	44°29'	110°10'	9/26/79	at US 20		-133
R82-75	Clear Creek	2,560	44°29'	110°10'	10/3/82	at US 20		-142
				PITCHSTONE PLATEAU AND SNAKE R. DRAINAGE—*PITCHSTONE PLATEAU*				
R82-45	North Boone Creek	1,950	44°06'	110°56'	9/29/82	at Reclamation road (snowing)	4	-137
R82-46	Calf Creek	2,200	44°08'	110°53'	9/29/82	at Reclamation road (1 ft snow on ground)	3	-136
R82-49	Glade Creek	2,200	44°07'	110°47'	9/29/82	at Reclamation road (Lakes in Drainage)	3	-132
R82-58	Rock Creek	1,930	44°07'	111°06'	9/29/82	at Cave Falls road	6	-131

Table 4. δD of cold waters in Yellowstone National Park and adjacent areas—*Continued*.

Sample	Name	Elevation (meters)	Latitude (N.)	Longitude (W.)	Date (mo/day/yr)	Location	Temperature (°C)	δD (‰)
PITCHSTONE PLATEAU AND SNAKE R. DRAINAGE—*PITCHSTONE PLATEAU—Continued*								
R82-59	Beaver Creek	1,800	44°07'	111°08'	9/29/82	at Cave Falls road	6.5	-133
R82-60	Robinson Creek	1,740	44°08'	111°10'	9/29/82	at end of Sawmill Creek road	10	-133
R82-61	Porcupine Creek	1,710	44°05'	111°13'	9/29/82	at Cave Falls road		-132
R82-73	Snow Creek	2,070	44°15'	111°06'	10/1/82	at Park boundary road 509	7	-135
R82-74	North Fork Partridge Creek	2,290	44°20'	111°09'	10/1/82	1 mile north of Snow Creek at Park boundary	3	-135
PITCHSTONE PLATEAU AND SNAKE R. DRAINAGE—*BECHLER RIVER*								
R82-62	Bechler River	2,130	44°15'	110°56'	9/30/82	at stock crossing of river	7	-134
R82-63	Bechler River area creek	2,130	44°15'	110°56'	9/30/82	small creek 100 yards from stock ford	5	-131
R82-64	Bechler River area spring	2,100	44°15'	110°56'	9/30/82	30-40 gallon/minute spring on Bechler trail	6	-134
R82-65	Bechler River area spring	2,040	44°15'	110°56'	9/30/82	14 gallon/minute spring Bechler trail	4	-132
R82-66	Bechler River area spring	2,010	44°15'	110°56'	9/30/82	3 gallon/minute spring Bechler trail	3.5	-134
R82-69	Bechler River area spring	1,980	44°14'	110°57'	9/30/82	spring near fall tree fishing hole	4	-135
R82-72	Boundary Creek	1,890	44°11'	111°00'	9/30/82	at south edge of Bechler Meadow		-136
PITCHSTONE PLATEAU AND SNAKE R. DRAINAGE—*SHOSHONE LAKE AREA*								
T73-20	Grants Pass Spring	2,410	44°23'	110°49'	9/00/73	at Grant Pass on Howard Eaton trail		-135
W-804	Grants Pass Spring	2,410	44°23'	110°49'	10/4/76	at Grant Pass on Howard Eaton trail		-143
T73-87	Shoshone Fall Creek	2,410	44°23'	110°47'	9/00/73	above thermal area		-130
PITCHSTONE PLATEAU AND SNAKE R. DRAINAGE—*HEART LAKE AREA*								
T78-38	North Fork of Witch Creek	2,320	44°18'	110°30'	10/4/78	at Fissure group		-137
T78-39	South Fork of Witch Creek	2,320	44°18'	110°30'	10/4/78	at Fissure group		-142
T78-44	Witch Creek	2,320	44°17'	110°32'	10/4/78	above all thermal springs		-140
PITCHSTONE PLATEAU AND SNAKE R. DRAINAGE—*SNAKE RIVER AREA*								
R78-43	Snake River	2,070	44°06'	110°40'	10/6/78	at bridge on US 89		-136
R82-1	Snake River	2,070	44°06'	110°40'	9/21/82	at bridge on US 89	11	-133
R82-50	Snake River	2,070	44°06'	110°40'	9/29/82	at bridge on US 89	8	-132
R90-1	Snake River	2,070	44°06'	110°40'	9/9/90	at bridge on US 89	17	-131
R82-51	Crawfish Creek	1,950	44°09'	110°41'	9/29/82	above Moose Falls on US 89	14	-139
R82-52	Polecat Creek	2,070	44°07'	110°42'	9/29/82	1 mile west of Flagg Ranch	14	-126

short distances with minimum evaporation. Those streams are likely to have temperatures only slightly higher than that of the ground water. Even on warm days in the Yellowstone region, temperatures of streams were seldom observed to be more than 10°C higher than temperatures recorded in local cold springs, and the δD of the streams did not change during the day as their temperatures rose. Such streams are the most likely streams to have fairly uniform δD values from year to year when sampled in the fall at times that specifically avoid major storms.

Isolating the effect of possible evaporation on the δD of stream water is difficult in mountainous regions because the inflow is from many inconspicuous sources along the courses of the streams. Where gradients are steep, the water comes from a range of altitudes, possibly with different isotopic compositions. However, evaporation is expected to be limited at the low temperatures of the springs and within the short average distances of flow from the springs to our sampling points. This assumption is supported by the clustering of data around the GMWL in figure 5 and by isotope studies of rivers (Friedman and others, 1964; Fritz, 1981) that have shown that flowing water in temperate climates normally undergoes very little change in δD due to evaporation. Even the Nile River undergoes a δD increase of only 3 ‰ during its 2,900-km journey from source to ocean (Friedman and others, 1964). Thus, it is not surprising that we observed no change in δD of the Stillwater River in sample sites 65 km apart (table 4).

Lake water, however, with a long residence time, generally shows significant increases in δD and $\delta^{18}O$ due to evaporation (Friedman and others, 1964; Gat, 1981). The compositions of lake waters in figure 5 plot on a typical evaporation trend. The difference in δD values between Yellowstone Lake (–128 to –133 ‰) and the average of accessible inflowing streams (–135 ‰) is due largely to evaporation. The isotopic change occurs over the 10-year average residence time (Pearson and Truesdell, 1978) of water in Yellowstone Lake. In order to minimize possible effects of evaporation, we avoided streams that traversed standing bodies of water, such as lakes, or that received significant inflow from swampy meadows.

Results: δD of Surface Water in the Greater Yellowstone Area

The δD values of nearly 300 water samples from cold springs, wells, cold creeks, and rivers, collected from 1967 to 1990, and their locations are listed in table 4. More detailed locations, on U.S. Geological Survey Yellowstone National Park or quadrangle topographic maps, can be obtained from the information in table 4. General sample locations, δD values, and pertinent physiographic features are shown in figure 7.

Areas North of the Park

In 1979, streams draining Precambrian to Mesozoic volcanic, igneous, and sedimentary rocks of the Gallatin and Madison Ranges north and west of the Park were sampled from Highway 191 along the Gallatin River drainage for nearly 40 km north of the Park. The highest peaks are higher than 3,350 m (11,000 ft) altitude, and steams flowing into the Gallatin River have steep gradients to the sampling points at 1,525–1,825 m (5,000–6,000 ft) altitude. The δD values of most streams ranged from –144 to –147 ‰. A spring a short distance outside of the Park had a δD value of –152 ‰, and a spring 40 km north of the Park boundary had a value of –149 ‰, differing considerably from values of nearby streams. These springs have not been sampled over a time interval to determine whether the lower δD values reflect recharge at higher altitudes than the inflow for the streams or ephemeral recharge from the last storm in the area.

The Absaroka Mountains to the north of the Park between the Yellowstone and Boulder-Stillwater Rivers are characterized by volcanic and Precambrian terrain. That area was sampled in a road traverse in 1978. Much of the area is higher than 3,050 m (10,000 ft) altitude; samples were collected from altitudes of 1,525–2,450 m (5,000–8,000 ft) from streams with steep gradients. The δD values of most of the sampled streams near the Park ranged from –144 to –149 ‰. The δD values of water in the Stillwater River and its tributaries did not vary significantly over a distance of nearly 65 km and over an altitude change of 1,225 m (4,000 ft) before the Stillwater flowed into the Yellowstone River suggesting that, for this stream, typical of those we studied, evaporation and mixing of water from different altitudes had minimal effect on δD values. In 1978, the Montanapolis warm spring had a δD value of –153 ‰, 6–10 ‰ lower than the value of local recharge in the area. This spring possibly was recharged during a colder climate than the nearby cold streams and was warmed by deep circulation. The low δD value of this warm spring, relative to local recharge water, is consistent with a similar relationship of δD values for water from deep warm wells and springs, relative to local recharge water in an area from southeastern California to the Snake River Plain in southern Idaho (Smith and others, 2002). As pointed out by these authors, the water in these wells was probably recharged during Pleistocene glaciation.

The area north of the Park between the Stillwater River and U.S. Highway 212 contains the Beartooth Wilderness Area with peaks higher than 3,650 m (12,000 ft) chiefly composed of Precambrian rocks. Suitable sampling sites were limited along the road traverse because many drainages in the high country contain glacial lakes. However, the sampled streams and rivers adjacent to the Beartooth Range have a remarkably narrow range of δD values (–137 to –141 ‰). The single spring sampled had a lower δD value of –144 ‰. The δD values of streams in the Beartooth region are higher (less negative) than those farther west in the Absaroka and Gallatin Ranges.

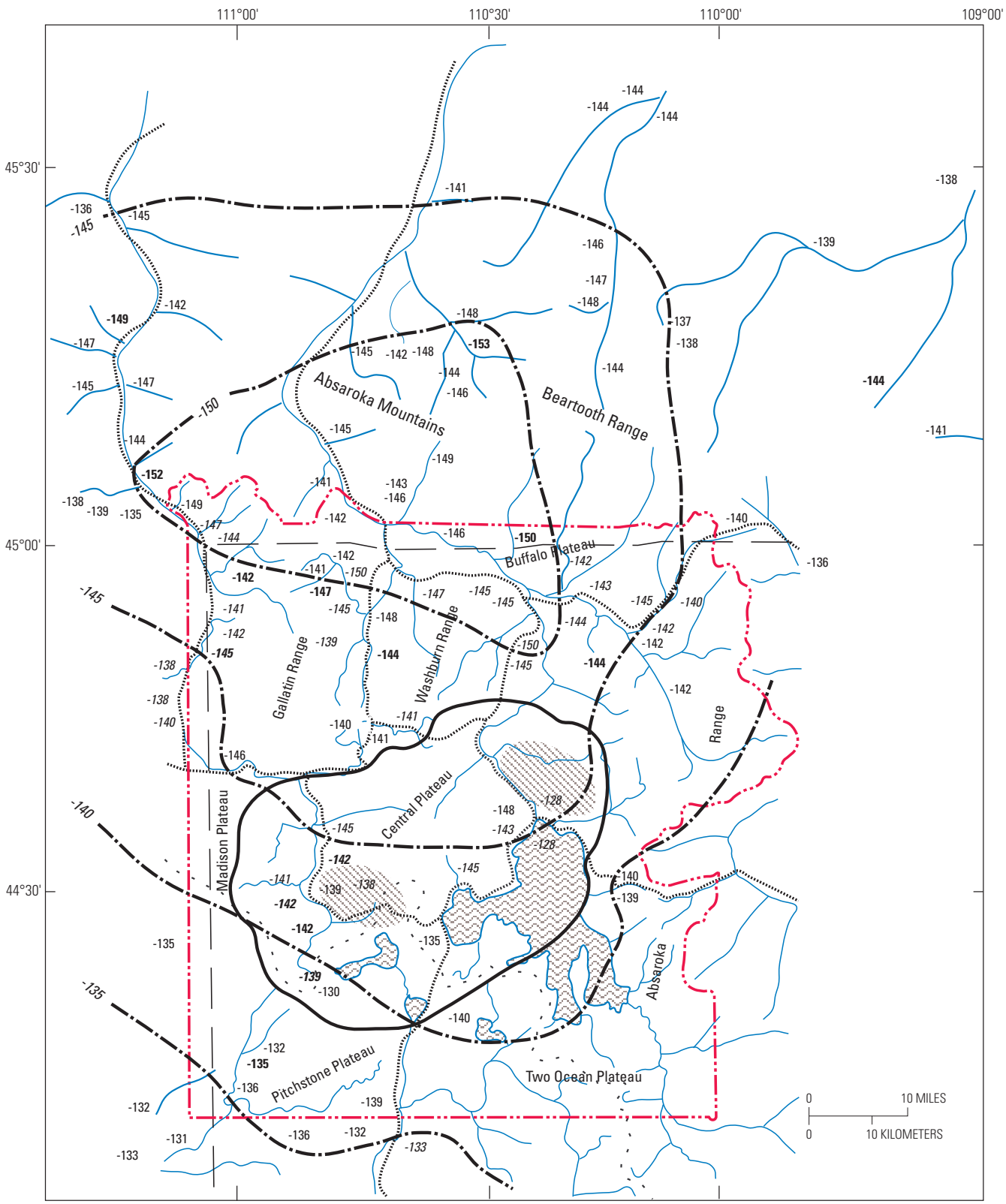

Figure 7. Sketch map of Yellowstone National Park and adjacent area showing select topographic features and the δD of cold waters at each sample site. The δD values are plotted in the general vicinity of sample sites. For detailed locations see table 4. Bold numbers indicate samples of springs and wells. Italics indicate average values for several years. Plain numbers indicate only one sample analyzed. Contours (dot dashed lines) are drawn around the most negative δD values, guided by values for samples believed to be most representative of infiltrating waters. See figure 1 for meaning of other lines and patterns.

Gallatin Range

The Gallatin Range in the northwestern part of the Park is bounded by the Gallatin River on the west, the Gardiner River on the northeast, and the Madison River on the south. The range contains some of the highest altitudes and the largest area of high mountains in the Park. On the north side, δD values from the Gardiner River ranged from –140 to –147 ‰, whereas δD values from Glen Creek (sampled almost yearly from 1970 to 1990) ranged from –147 to –153 ‰. In 1990, the δD value of (east) Fawn Creek was –141 ‰, whereas values from springs along the north and south sides of the creek were –146 to –147 ‰. On the west side, δD values of Daly, Black Butte, Specimen, Fan, and (west) Fawn Creeks ranged from –139 to –151 ‰. In 1990, the δD values of springs along the south side of (east) Fawn Creek were –142 to –145 ‰. The δD value of cold streams in the southern part of the range were less negative (–135 to –142 ‰), based on data from Duck, Cougar, Panther, and Indian Creeks. A small spring with variable flow near Grayling Creek has δD values of –136 to –147 ‰. It appears that, for a given year, the δD values of the fall stream discharges from the northern Gallatin Range are an average of about 5 ‰ lower than those from the southern part of the range.

Washburn Range

The Washburn Range, north of the caldera and including the area surrounded by the northern loop of the Yellowstone Highway, contains watersheds that drain into the Gardiner, Gibbon, and Yellowstone Rivers. This area includes Mount Washburn, with an altitude higher than 3,100 m (10,200 ft). On the north side of the range, Lava, Blacktail Deer, Elk, and Tower Creeks had δD values from –143 to –148 ‰, whereas Antelope Creek, on the east side of the range, which is probably recharged at higher altitudes on Mount Washburn, had lower δD values (from –147 to –153 ‰). This is one of the few cases in which we observed clear variation of δD with altitude for inflow in a given basin. The δD values of the Gibbon River above Virginia Meadows ranged from –140 to –143 ‰, consistent with an increase in the δD values of surface waters to the south.

Buffalo Plateau

The Buffalo Plateau is north of the Yellowstone and Lamar Rivers and Slough Creek, and it extends outside the Park. The highest altitudes are higher than 3,050 m (10,000 ft) largely on Precambrian rocks. A small, but fast moving, cold stream draining the high plateau had a δD value of –150 ‰ in 1977. Slough Creek, Little Cottonwood Creek, and Buffalo Creek had δD values of –140 to –146 ‰ from 1977 to 1990.

Absaroka Range

The Absaroka Range is a large north-south-trending chain of mountains in the entire eastern part of the Park and north of the Park where it joins the Beartooth Wilderness Area on the east and the Gallatin National Forest region on the west. Along the eastern margin of the Park, the Absaroka Range consists of intermediate-silica volcanics—remnants of Eocene stratovolcanoes. Topography is steep, and peaks along the ridge of the range are commonly higher than 3,050 m (10,000 ft). The δD values from streams in the Lamar River–Soda Butte drainage ranged from –139 to –144 ‰, with an average value of –142 ‰. In the area near Sylvan Pass, δD values from Cub Creek ranged from –133 to –142 ‰, with an average value of –139 ‰. The streams near Sylvan Pass were sampled at altitudes from higher than 2,600 m (8,500 ft) to lower than 2,200 m (7,200 ft). It is clear that δD values of small streams decrease from south to north, as was the case on the Central Plateau to the west.

Madison Plateau

The Madison Plateau along the rim of the Yellowstone caldera is composed of Plateau Rhyolite. The highest surfaces are slightly higher than 2,550 m (8,400 ft) altitude. Discharge from this plateau was sampled at three sites from 1971 to 1990: a cold spring at the base of rhyolite cliffs about 3 km west of Old Faithful Geyser, the Little Firehole River above Mystic Falls, and a cold spring adjacent to the old road to Lonestar Geyser. The total range of δD values during the 11-year collection interval for these waters was only –139 to –143 ‰. The cold spring at Grants Pass on the Howard Eaton trail to Shoshone Lake, which could be recharged on the Madison Plateau or to the east in the hills north of Shoshone Lake, had δD values of –135 ‰ in 1973 and –143 ‰ in 1976. Values from cold springs in the vicinity of Shoshone Geyser Basin ranged from –135 to –138 ‰. The δD of the subsurface discharge appears to decrease slightly from south to north in the plateau area.

Central Plateau

The Central Plateau borders the major geyser basins and covers the western resurgent dome of the Yellowstone caldera. The highest altitudes on the Central Plateau are about 2,625 m (8,600 ft), and much of the plateau is higher than 2,550 m (8,400 ft). Nez Perce Creek, which drains the largest watershed in the Central Plateau, was sampled at an altitude of about 2,200 m (7,200 ft). δD values of –143 to –147 ‰ were measured from 1971 to 1990. The values are within the –143 to –148 ‰ range observed from 1975 to 1982 for Arnica Creek, which has a much steeper gradient, near the southeastern margin of the Central Plateau. δD values of –140 to –148 ‰ were obtained between 1971 and

1990 for unnamed creeks with steep gradients draining the 2,625-m (8,600-ft) altitude Elephant Back Mountain on the east side of the plateau. The δD values of the Gibbon River, which has some tributaries on the north margin of the Central Plateau, ranged from –140 to –144 ‰ from 1967 to 1990. The δD values of cold streams and wells on the west margin of the Central Plateau were slightly less negative. On the west margin of the plateau, the δD values of water from cold wells for water supplies at the Midway picnic ground in Lower Geyser Basin and at the Old Faithful and Norris Geyser Basins ranged from –138 to –143 ‰. Substantially higher δD values were obtained from streams on the south margin of the plateau. DeLacy Creek has a small drainage starting at about 2,550 m (8,400 ft) altitude. δD values of DeLacy Creek ranged from –136 to –142 ‰ during a 20-year period. Even less negative values of –133 to –137 ‰ were obtained for Little Thumb Creek that drains similar altitudes about 8 km east of DeLacy Creek. The δD values of all discharge from the central, northern, and eastern margins of the Central Plateau ranged from –138 to –148 ‰, and they averaged about –143 to –145 ‰. The δD values of discharge from the south margin were about 5–7 ‰ greater.

Yellowstone Lake and Yellowstone River

The δD values of Yellowstone Lake water at the outlet to the Yellowstone River near Fishing Bridge and at Pumice and Steamboat Points were measured between 1975 and 1990 at –128 to –133 ‰. The δD value of the Yellowstone River at Buffalo Ford was –125 to –130 ‰. The enrichment of this water in deuterium relative to water in inflow streams reflects evaporation in the lake. This enrichment is not surprising because the residence time of water in the lake is about 10 years (Pearson and Truesdell, 1978).

Mirror Plateau

The Mirror Plateau borders the fumarolic thermal areas east of the Yellowstone caldera. The highest altitudes are higher than 2,900 m (9,600 ft), and much of the plateau is higher than 2,675 m (8,800 ft). Most of the streams sampled are in steep drainages, and δD values should be representative of discharging springs in the area. Streams from the Mirror Plateau and Specimen Ridge had δD values of –143 to –145 ‰ between 1975 and 1990. These values are similar to those from the streams and rivers draining the Absaroka Range to the east and north and the Central Plateau to the west during a longer period of time. Most of the Mirror Plateau drainage flows north into the Yellowstone River along its Grand Canyon.

Pitchstone Plateau and Areas South and West of the Park

The Pitchstone Plateau is southwest of the caldera at altitudes as high as 2,675 m (8,800 ft). Springs that probably recharged on the plateau were sampled in 1982 at altitudes below 2,050 m (6,800 ft) during a single traverse along the trail on the east side of the Bechler River. δD values of the water from the springs ranged from –132 to –135 ‰, similar to values observed for the Bechler River (–134 ‰). The δD values of streams and rivers areas south (Boone, Calf, and Glade Creeks) and west (Strong, Rock, Beaver, and Robinson Creeks) of the Pitchstone Plateau outside of the Park, also sampled in 1982, have essentially the same range of δD (–131 to –137 ‰). These values are clearly less negative than those obtained from streams in the Central and Madison Plateaus to the north.

Snake River Drainage

We have not sampled the Two Ocean Plateau between the Snake and Yellowstone Rivers. However, δD values increased southward in the Park, and no cold streams or springs with δD values lower than –144 ‰ were obtained from waters south of lat 44°30'N. Cold springs in the Shoshone Geyser Basin ranged from –135 to –138 ‰ in 1973. Witches Creek, above the thermal springs at Heart Lake, had a δD value of –140 ‰ in 1978. The cold spring at Grants Pass on the Howard Eaton trail to Shoshone Lake, which could be recharged on the Madison Plateau or to the east in the hills north of Shoshone Lake, had δD values of –135 ‰ in 1973 and –143 ‰ in 1976. The Snake River at Flagg Ranch had δD values of –131 to –136 ‰ from 1978 to 1990.

Discussion

δD values of the cold-water samples for Yellowstone National Park and surrounding areas given in table 4 are summarized in figure 7. Five relationships are evident from the data in figure 7: (1) δD values of surface water north of the Park and in the northern part of the Park become more negative from south to north and from east to west, (2) δD values of surface water more negative than –144 ‰ are not present in the southern half of the Park, (3) except for two small cold streams (both of which probably are influenced by local storms), surface waters with δD values of –148 to –150 ‰ are not found near the geyser basins, (4) localities where the δD values of streams or springs are ≤ –150 ‰ are exclusively north of the caldera and are relatively scarce, and (5) the lowest δD value for a warm sinter-depositing spring (Montanapolis) north of the Park is lower than local recharge and lower than the value modeled for the deep thermal water in the Park.

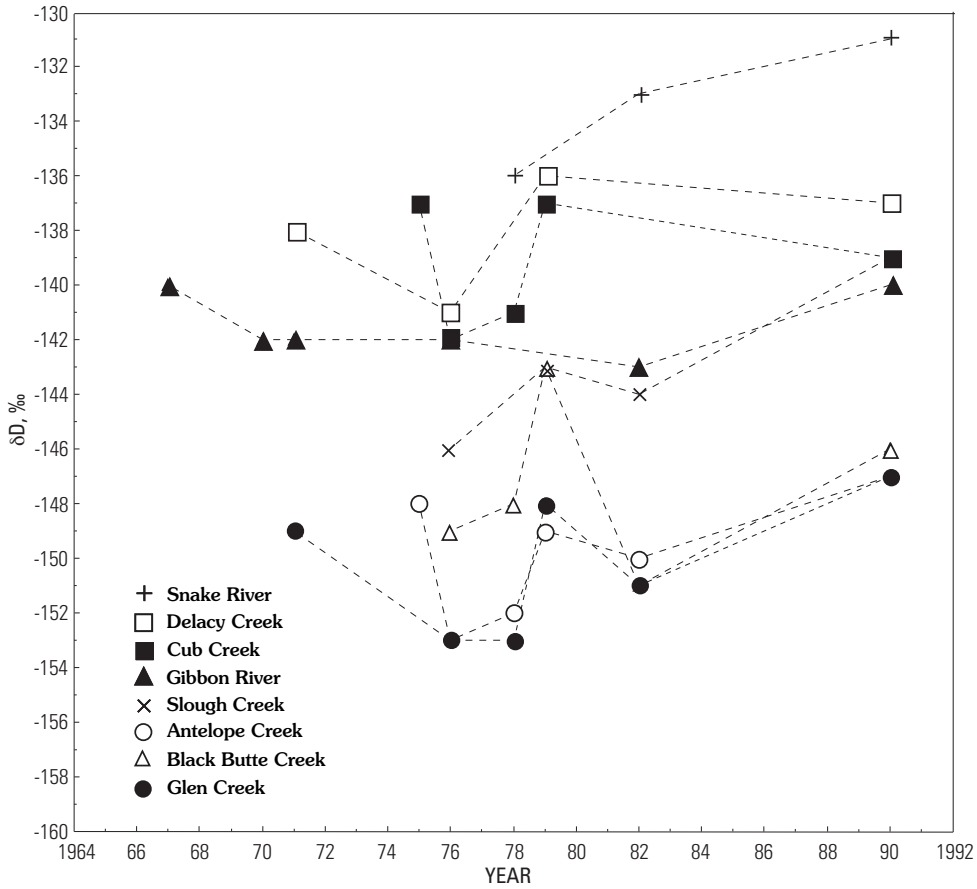

Figure 8. Yearly variations in δD of fall-season discharge of eight Yellowstone National Park streams sampled repeatedly from 1967 to 1990.

Yearly Variations in δD Values at Individual Sites

The pattern of δD distribution for cold waters in the Park, developed in the course of our study, is dependent in part on analyses of water from sites collected only once or twice. In order to determine if δD values from a specific site were consistent from year to year and if the same relative differences between waters from different locations persisted in different years, we collected samples from selected accessible sites during a span of years.

The maximum variation in δD for an individual stream over the collection period from 1967 to 1990 was 8 ‰. Although there were exceptions, the δD values of most streams varied by about the same amount from year to year. This pattern is illustrated in figure 8, which shows similar patterns for δD variations of eight representative streams at different locations in the Park from 1967 to 1990. The important point is that the average δD value for each locality provides a valid picture of the spatial variations in δD of possible infiltrating waters.

Our database is not sufficient to permit us to understand all of the factors controlling the detailed δD of precipitation in the area. A detailed understanding must await data for individual storms, collected over an extended period of time, and information on the residence times of infiltrating precipitation that recharges the streams. As indicated in figure 8, the least negative δD values are for stream samples collected in 1990, whereas the most negative values are for stream samples collected in 1976. The late 1980s were characterized by below normal winter precipitation, whereas the early 1970s were characterized by above normal winter precipitation, as indicated by the yearly average discharge of major rivers in the Yellowstone region (Norton and Friedman, 1991). Although most of the fall stream flow was recharged during the previous spring runoff, possibly a substantial component remained from previous years. Much more detailed studies are needed; however, the average δD values of the streams for a given year apparently correlate with the winter precipitation in the preceding year.

Source of Recharge of Deep Thermal Water If It Occurred During the Holocene

For a system in which the deep thermal water has a short residence time and whose composition responds rapidly to changes in climate, possible recharge areas are constrained by low δD values (–148 to –150 ‰) comparable to those of the deep thermal waters. If the deep thermal water was recharged under the present climatic conditions, the location of recharge must have been in the mountainous areas north and northwest of the caldera. These include (1) the Gallatin Range in the northwest part of the Park and north of the Park between the Gallatin

and Yellowstone Rivers, (2) the Washburn Range, (3) the Buffalo Plateau, and (4) the Absaroka Mountains north of the Park.

From geologic considerations (figs. 9 and 10), the most likely recharge area for deep thermal water underlying the geyser basins on the west side of the caldera is the Gallatin Range between Highways 191 and 89 in the northwestern part of the Park and probably extensions of that range north of the Park. This high-altitude area is bounded by several major north-south-trending faults (fig. 9) that parallel regional faults known from earthquake data to be active (Christiansen, 1984; Pitt, 1987; Pierce and others, 1991; Smith and Rubin, 1994). Large segments of the faults are covered by glacial till and river gravel that are excellent aquifers for recharge of water along the faults to deep levels. Runoff from snowmelt in the spring supplies water to the gravel and that water can infiltrate along the faults to deep levels of the Yellowstone thermal areas. This area also is characterized by large areas of fractured Precambrian basement, Paleozoic and Mesozoic sedimentary rocks with karst topography in limestones, and Eocene volcanics that possibly have permeable contacts. Recharge water may also flow along some northwest-southeast-trending faults in the northwest part of the Park. Those faults parallel major active faults west of the Park (Holdahl and Dzurisin, 1991). Additional recharge could come from the Washburn Range, but, because faults in the Yellowstone Tuff also are oriented north-south, water from this area is more likely to recharge the gas-rich thermal areas on the east side of the caldera. Tectonic and sedimentary structures on the east side of the caldera do not favor recharge from the Absaroka Mountains to the east. The recharge area for deep thermal waters in the Gallatin Range is at least 20 km from outflow at Norris Geyser Basin, 30 km from the outflow at Lower Geyser Basin, and as far as 60–70 km from outflow at the Shoshone and Heart Lake Geyser Basins, respectively. Such distances for deep recharge indicate the presence of an extremely large hydrothermal system. However, these distances are consistent with the size of fossil systems inferred from isotope studies to have been driven by large plutons (Taylor, 1986; Criss and Taylor, 1986).

We need to consider whether precipitation in the Gallatin Range is sufficient to recharge the deep reservoir that supplies the geyser basins on the west side of the caldera. Measured discharge rates of the rivers and chloride concentrations in river waters have been used to calculate the rate of total discharge of the deep component of the hot-spring waters (Fournier, 1989; Norton and Friedman, 1991; Friedman and Norton, this volume). The amount of deep water (that is, water heated to ≥350°C and having 360 ppm Cl) from the west side of the caldera, measured by the chloride flux (Norton and Friedman, 1991; Friedman and Norton, this volume) in the Madison and Snake Rivers, averages about 7.5×10^{10} kg/yr of water with nearly 90 percent derived from the Madison River. The map area of the Gallatin Range in the Park between Highways 191 and 89 is about 1,000 km^2, of which about 400 km^2 is above 2,550 m (8,400 ft) altitude. The annual mean precipitation at West Yellowstone and Old Faithful is about 75 cm/yr on the basis of precipitation summaries by Dirks and Martner (1982). Much more precipitation is expected at altitudes higher than 2,550 m (8,400 ft) in the Gallatin Range. Indeed, precipitation summaries by Dirks and Martner (1982) indicate that the annual mean precipitation in the Gallatin Range is close to 150 cm; most of it is winter snow. Thus, probably 6×10^{11} kg/yr of precipitation falls on the high altitudes of the Gallatin Range within the Park. The amount of runoff from the topographically high areas of the Gallatin Range within the Park is approximately eight times the 7.5×10^{10} kg/yr of deep water estimated to be discharged from the thermal basins on the west side of the caldera each year (Norton and Friedman, 1991; Friedman and Norton, this volume). Additional recharge could be received from the extension of this possible recharge area to the north and northwest of the Park.

The watershed where δD of cold waters is –150 ‰ is limited to the northernmost Gallatin Range, and it does not appear to be large enough to recharge the deep levels of the thermal areas on the west side of the caldera. Furthermore, the δD of much of the possible infiltrating cold water in the southern part of the Gallatin Range is less negative than –148 ‰. Consequently, there is not enough infiltrating cold water of the right composition in the Gallatin Range to account for all of the deep thermal water on the west side of the caldera. This possibly indicates that some recharge is received from ranges east of the Gallatin Range or, more likely, that the deep thermal water was recharged during a colder time interval during which there was greater winter snow accumulations and lower δD values of precipitation. Judging from variations observed in figure 8, we expect δD values of precipitation to be quite sensitive to increases in snowfall. High snowfall accumulations are recorded for the Yellowstone region near the end of the 19th century (Dirks and Martner, 1982), and they also are expected to have occurred during prolonged cold periods such as those observed in Europe in the 15th, 17th, and 18th centuries (Ferronsky and others, 1983). Of course the δD of precipitation was low during the Pleistocene when a large ice cap covered the Yellowstone Plateau as late as 15,000 years ago, and alpine glaciers were active until 11,000 years ago (Pierce, 1979).

Volume of Deep Thermal Water in the Western Side of the Caldera

A schematic north-south cross section through the west side of the caldera (fig. 10) shows hot-spring activity and inferred recharge of local shallow and deep thermal waters. According to R.L. Christiansen (written commun., 1990), the caldera consists of cylindrical cores that originally collapsed and later formed the resurgent domes with shallow tensional faults. The resurgent domes are surrounded by a thick zone of steeply dipping concentric faults that form the main ring-fracture zone of the caldera. The outer part of the caldera consists of large slump blocks that extend along shallow faults to the structural wall of the caldera. The locations of hot-spring activity in Yellowstone probably are controlled primarily by

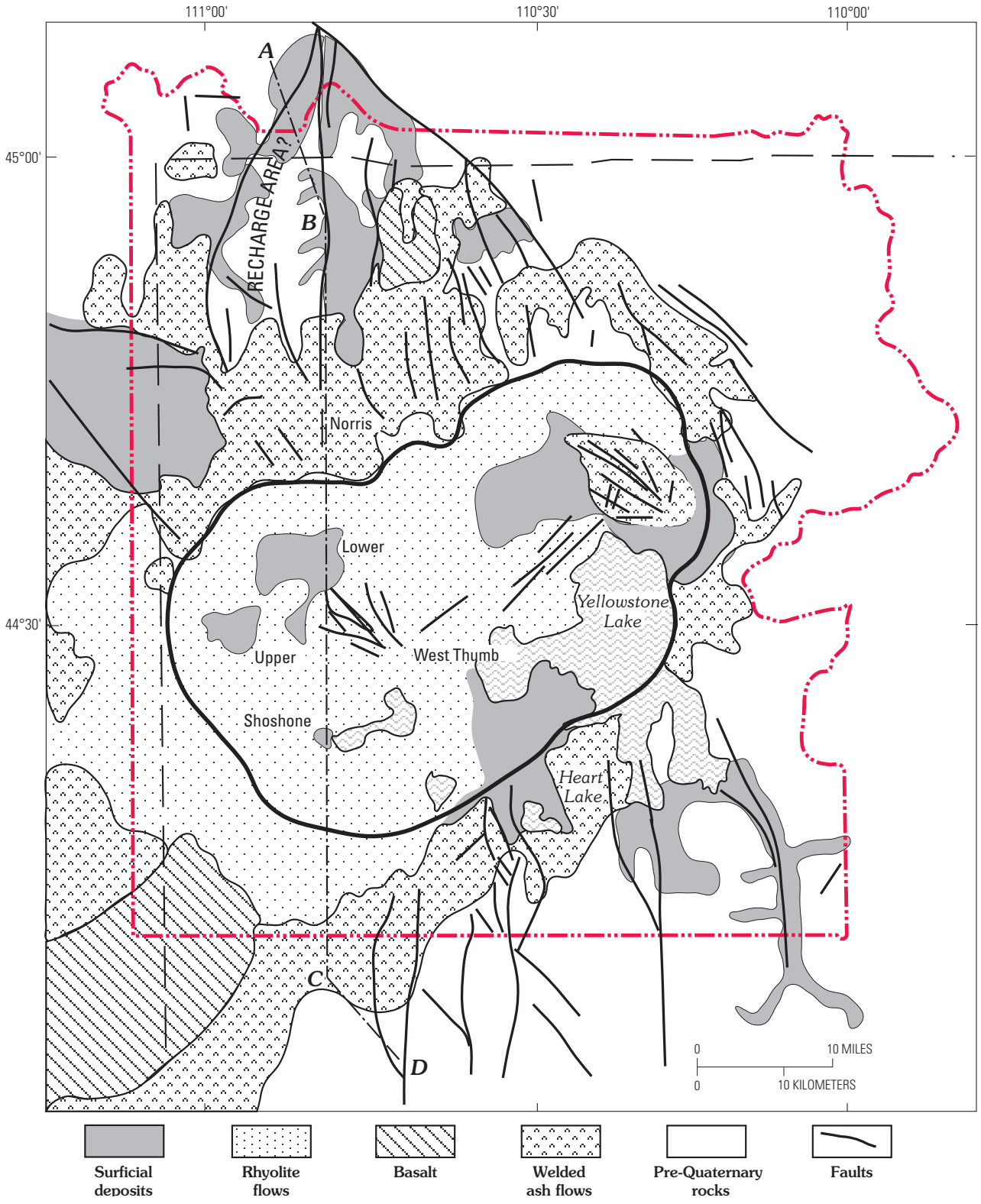

Figure 9. Geologic sketch map of Yellowstone National Park showing possible recharge area for deep thermal waters of the geyser basins on the basis of δD values of cold waters in figure 7. Also shown (dashed dot line ABCD) is location of cross section in figure 10. The area marked RECHARGE AREA? is the center of the most likely source of recharge for thermal waters at Norris, Lower, and Upper Geyser Basins and possibly more distal geyser basins at West Thumb, Shoshone, and Heart Lake. If the deep water contains a component of Pleistocene water and is well mixed, the recharge could be much closer to the caldera inside the Park. See figure 1 for meaning of other lines and patterns.

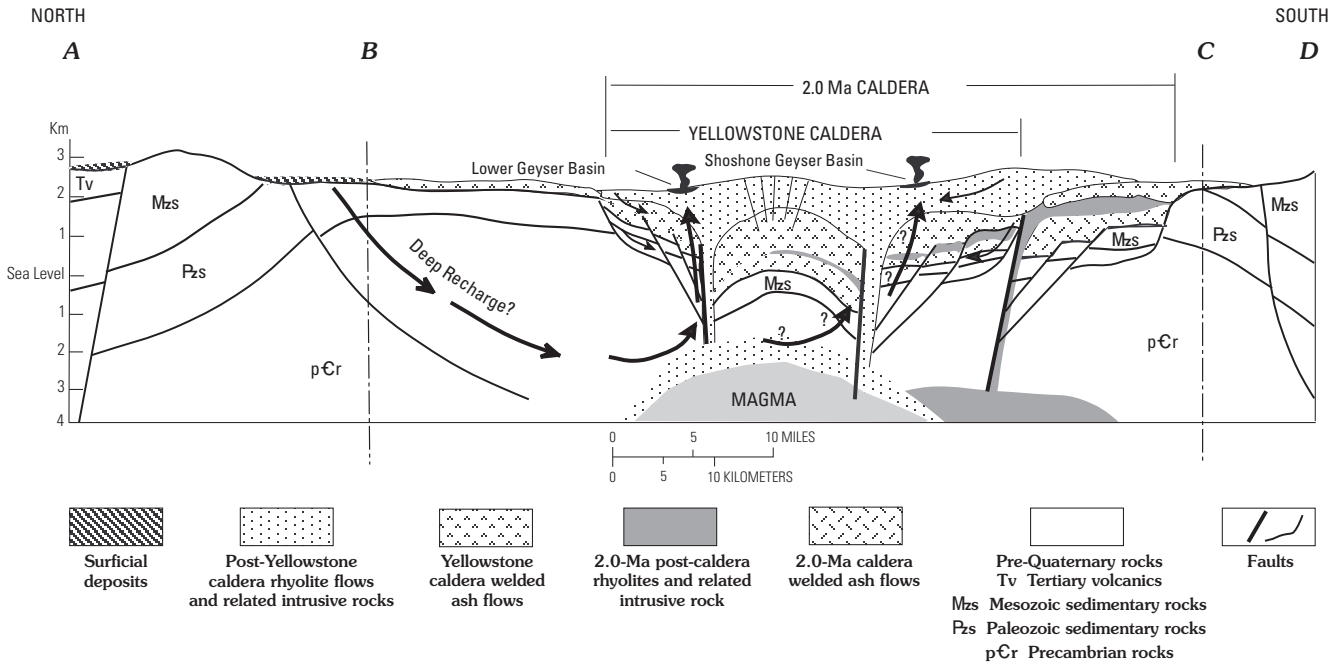

Figure 10. Schematic north-south cross section through the west side of Yellowstone National Park (along ABCD line in fig. 9) showing possible recharge for deep thermal water and shallow mixing waters at Lower and Shoshone Geyser Basins. Caldera structure based on a sketch from R.L. Christiansen (written commun., 1990). The deep recharge is shown for a system in which the deep water has a short residence time and whose δD values respond rapidly to climate changes. If the deep water contains a component of Pleistocene water and is well mixed, the recharge could be much closer to the caldera.

the main ring-fracture faults that are related to the formation of the caldera and also to younger north-south faults inside and outside of the caldera. Individual springs, such as those at Upper and Lower Geyser Basins, however, may be along shallow faults that parallel those in the resurgent dome to the east. The shallow structures at the margins of the caldera probably permit a wedge of cold water to mix with deep thermal water within the caldera.

The maximum volume of the deep thermal-fluid reservoir in the west side of the caldera can be assumed to be the volume of a cylinder approximately 30 km in diameter, the diameter of the outer ring fracture of the caldera. The bottom of the reservoir is the lower limit of circulation of meteoric water, at which seismic activity maintains permeability in the rocks. This depth probably is about 4 km as indicated by the deepest focal depth of earthquakes beneath the caldera (Fournier and Pitt, 1985; Smith and Rubin, 1994; Fournier, 2000). Deeper circulation of water possibly took place in the past, and water possibly circulated into the magma during the recurrent explosive activity that occurred during and immediately after formation of the caldera (Hildreth and others, 1984). Today the circulation depth of meteoric water is probably limited by the depth at which rock deformation changes from primarily brittle-fracture to quasi-plastic flow (Fournier, 1989, 1991, 2000). This transition probably coincides with a thin zone of thermal cracking that migrates inward toward the magma with time as the rocks are cooled (Lister, 1974, 1983). Recharge of cold water along active faults possibly results in thermal cracking of intrusive rocks at depth creating a continuous supply of permeable rocks deep in the thermal areas (Christiansen, 1984). The top of the deep reservoir (defined as thermal water not influenced by shallow recharge) possibly extends in some areas to depths as shallow as 0.5 km, as indicated by the depth to the unmixed deep thermal water indicated from modeling (Truesdell and others, 1977) of the isotopic and chemical compositions of hot-spring waters. Thus, the maximum thickness of the reservoir for deep thermal water probably is about 4 km.

The maximum volume of water in this reservoir can be calculated if assumptions are made about the average porosity of the reservoir. The rocks in the caldera are a heterogeneous mixture of porous rhyolite flows, dense welded tuff, and some sediments from volcanic episodes. Studies of intracaldera volcanics associated with a smaller caldera at Long Valley, Calif., indicated porosities between 1 and 10 percent (Sorey and others, 1978). The higher figure probably is not realistic for the Yellowstone caldera because the Lava Creek and Huckleberry Ridge Tuffs are dense, and the deep thermal water is concentrated in highly fractured and permeable rhyolite and is not uniformly distributed throughout the caldera. The maximum average porosity for the intracaldera volcanics at Yellowstone is assumed to be about 5 percent (R.L. Christiansen, oral commun., 1991). Assuming an average porosity between 1 and 5 percent, the amount of thermal water in the deep reservoir on the west side of the caldera is between 28 and 141×10^{12} kg.

Age of the Deep Water

There are few constraints on the age of the deep water. The absence of such constraints leads to two possible models for the deep recharge. Pearson and Truesdell (1978) determined from tritium measurements that most of the thermal waters are mixtures of two waters—one containing tritium from an open, well-mixed reservoir of relatively short residence time, the other containing no detectable tritium, presumably derived from a deep source. The deep water contains no detectable tritium. Therefore, the deep water is at least 60 years old, based on the 12.3-year half life of tritium. Carbon-14 was not detected in CO_2 from fumarolic steam, as would be expected for a system swamped by CO_2 of igneous or sedimentary origin (F. J. Pearson, Jr., unpubl. data, 1978).

A maximum age of the deep water can be estimated from the discharge rate for deep water of about 7.5×10^{10} kg/yr, as measured from Cl inventory considerations (Norton and Friedman, 1991; Friedman and Norton, this volume) and from the estimates calculated above for the minimum and maximum volume of the deep water reservoir. The reservoir would be emptied in 370–1,900 years assuming a piston flow model in which water does not mix within the reservoir and assuming there is only one point of recharge. These times are generally consistent with the maximum time (1,150 years) for water-rock reaction estimated from a solution and recoil model for radium isotope supply to the hydrothermal system published by Clark and Turekian (1990). However, the times are not consistent with an age of at least 10,000 years based on He-4 flux measurements by Kennedy and others (1987, 1988). Such an old age is consistent with well-mixed models.

Are such recharge ages suggested by short residence times for the deep water hydrologically realistic? Fractured crystalline rocks generally have hydraulic conductivities in the range of 1 to 1×10^{-4} km/yr (deMarsily, 1986, p. 79). Clearly, the high end of this range is more than adequate to account for the proposed recharge of the deep thermal reservoir. The actual hydraulic conductivities are unknown. However, Caine and Forster (1999) calculated a similar range of conductivities for four representative types of fault-zone architectures. Fracture flow through uniformly fractured ignimbrites and flows or along major and continuous fault zones could provide the pathway for fluid recharge from the mountain ranges north of the caldera. However, not all major faults show field evidence of Quaternary activity (Pierce and others, 1991). Furthermore, based on preliminary flow modeling, special conditions are required to provide a flow path as long as that shown in figure 10 that does not break into a series of convection cells recharged from local waters (W.C. Shanks, oral commun., 1999).

Well-mixed models permit the possibility of older ages for the deep water. Also possible Pleistocene water has recently been discovered in warm-water wells and springs from southeastern California to southern Idaho. This water has consistently lower δD values than those of surrounding local recharge (Smith and others, 2002). A possible example of one of these springs is the sinter-producing warm spring (Montanapolis) in the Absaroka Range north of the Park. This spring has a δD of –153 ‰, about 5 per mil lower than that of local ground water. If the water from these springs and wells is proven to be Pleistocene in age, the time required to flush the entire deep reservoir of the Yellowstone hydrothermal system may be longer than 11,000 years.

Source of Recharge of Deep Thermal Water If a Substantial Component Remains from the Pleistocene

The present climate cycle is characterized by variable warm and cold periods (Vance and others, 1992; Feng and Epstein, 1993; Whitlock, 1993) and produces small but significant variations in the δD of precipitation. During the Pleistocene, the variations of δD of recharge water were probably much less than today as most of Yellowstone National Park, particularly the topographically high northern areas, was buried by thick ice (Pierce, 1979). The presence of thermal kanes indicates that some of the hot springs were flowing during the last glacial period. Given the fact that ice caps and glaciers commonly have a layer of water at their base (Patterson, 1981), the meteoric-water hydrologic head on the thermal system was probably much larger than today. The δD of recharge from glacier meltwaters underneath the ice cap during the Pleistocene likely was isotopically uniform, and it possibly had a value of about –160 ‰, similar to the value of the deep, warm, well water observed in southern Idaho (Smith and others, 2002). The contribution of chloride to the deep reservoir during the Pleistocene was probably the same as it is today. The uniformity of temperature, chloride, and δD in the deep thermal water indicates that the deep water probably has a uniform source of heat and chloride. The uniform chloride source could be produced by thermal-stress cracking and leaching by meteoric water of chloride from the freshly exposed rock (Lister, 1974; Christiansen, 1984; White and others, 1992) or by contribution from a magma across a brine-meteoric water interface (Fournier, 1989).

If the deep reservoir contains a component of Pleistocene water and if it is well mixed, the current deep recharge could have δD values as large as –140 to –145 ‰ depending on the size of the deep reservoir and the residence time of water in the reservoir. Waters of such composition could enter the deep system at geologically favorable sites around the caldera (fig. 9). Large uncertainties currently exist about the size of the deep reservoir on the west side of the caldera because it may be connected to the deep reservoir on the east side. Until more is known about the age, residence time, and mixing rates of the deep thermal water, the simplest interpretation is that most recharge for the deep thermal water in the west part of the Park is likely in the Gallatin Range within and northwest of the Park.

Conclusions

An extensive Park-wide program of collection and analysis of cold-water samples was undertaken to determine the sources of recharge to the deep thermal water underlying the geyser and hot-spring basins of Yellowstone National Park. Earlier chemical and isotopic modeling of boiling and mixing processes, as well as the compositions of waters from 200- to 300-m-deep drill holes, showed that δD of deep thermal water (–148 to –150 ‰) is significantly lower than that of local cold waters that enter thermal reservoirs only near the surface. Cold waters in the central, southern, and eastern parts of the Park are isotopically too heavy (generally δD = –130 to –144 ‰) to provide deep recharge. The deep water is at least 60 years old on the basis of tritium measurements, but it could be younger than 1,900 years or older than 10,000 years depending on the model used for volume and flow calculations. For a deep reservoir whose water has a short residence time, only in the Gallatin Range in and northwest of the Park are cold-water δD values sufficiently low and geologic structures appropriate to carry recharging water into the deep caldera reservoir. In this model, the possible source of recharge for the deep thermal water is at least 20 km, and possibly as much as 70 km, from outflow areas. These distances require remarkable flow rates for recharge and a young age for the deep water. The volume of high-altitude infiltration with δD ≤ –148 ‰ in this area is not sufficient at present to match the measured thermal outflow as determined from chloride-flux studies. In this model, this shortfall requires that infiltrating waters were recharged during a period characterized by somewhat cooler climate with more winter snowfall that at present. Such conditions occurred during the Little Ice Age (in the 15th century). There is reason to believe, however, on the basis of data from warm springs and wells from southern Idaho to southern California, that the residence time for the deep water could be more than 10,000 years. If the deep water is well mixed, a portion of deep thermal water (δD = –160 ‰) may have been contributed during Pleistocene glaciation. Under such conditions, the δD for the present recharge for the deep thermal water could be as large as –140 to –145 ‰, and it could enter the deep system at a number of geologically favorable areas around the caldera.

Acknowledgments

Many people contributed to the logistics, sample collection, analyses, and discussions of this work in the nearly 25 years during which the project was conducted. We particularly thank Bob Christiansen, Tyler Coplen, Bob Fournier, Irving Friedman, Mark Huebner, Pat Muffler, Joe Pearson, Joe Whelan, and Don White of the U.S. Geological Survey; Wayne Hamilton and Rick Hutchinsen of the National Park Service; and many other visiting scientists, students, and spouses who joined us on the many memorable field trips in the Yellowstone area. We are particularly indebted to Pat Shanks for discussions regarding modeling of residence times of water in the deep reservoir. This study was recommended by Don White, who was a wonderful mentor to the authors when they were young scientists beginning to fathom the wonders of Yellowstone.

References Cited

Allen, E.T., and Day, A.L., 1935, Hot springs of the Yellowstone National Park: Carnegie Institution of Washington Publication 466, 525 p.

Bargar, K.E., and Dzurisin, Daniel, 1986, Bibliography and brief history of the studies by the U.S. Geological Survey in Yellowstone National Park, Wyoming, Idaho, and Montana: U.S. Geological Survey Open-File Report 86-573, 27 p.

Bryson, R.A., and Hare, F.K., 1974, Climates of North America, *in* Landsberg, H.E., ed., World survey of climatology: Amsterdam, Elsevier, p. 1–47.

Caine, J.S., and Forster, C.B., 1999, Fault zone architecture and fluid flow—Insights from field data and numerical modeling, *in* Haneberg, W.C., Mozley, P.S., Moore, J.C., and Goddwin, L.B., eds., Faults and subsurface fluid flow in the shallow crust: American Geophysical Union Geophysical Monograph 113, p. 101–127.

Christiansen, R.L., 1984, Yellowstone magmatic evolution—Its bearing on understanding large-volume explosive volcanism, *in* Explosive volcanism—Inception, evolution, and hazards: Washington, D.C., National Academy of Sciences (U.S. National Research Council Geophysics Study Committee), p. 84–95.

Clark, J.F., and Turekian, K.K., 1990, Time scale of hydrothermal water-rock reactions in Yellowstone National Park based on radium isotopes and radon: Journal of Volcanology and Geothermal Research, v. 40, p. 169–180.

Craig, Harmon, 1961, Standard for reporting concentrations of deuterium and oxygen-18 in natural waters: Science, v. 133, p. 1,833–1,834.

Craig, Harmon, Boato, Giovanni, and White, D.E., 1956, Isotope geochemistry of thermal waters: National Academy of Sciences, National Research Council Publication, v. 19, p. 29–39.

Criss, R.E., and Taylor, H.P., Jr., 1986, Meteoric-hydrothermal systems, *in* Valley, J.W., Taylor, H.P., and O'Neil, J.R., eds., Stable isotopes in high temperature geologic processes: Reviews in Mineralogy, v. 16, p. 373–424.

deMarsily, Ghislain, 1986, Quantitative hydrogeology: San Diego, Calif., Academic Press, 440 p.

Despain, D.G., 1987, The two climates of Yellowstone National Park: Montana Academy of Science Proceedings, v. 47, p. 11–19.

Dirks, R.A., and Martner, B.E., 1982, The climate of Yellowstone and Grand Teton National Parks: U. S. Department of Agriculture, National Park Service, Occasional paper no. 6, 26 p.

Dzurisin, Daniel, Savage, J.C., and Fournier, R.O., 1990, Recent crustal subsidence at Yellowstone caldera, Wyoming: Bulletin of Volcanology, v. 52, p. 247–270.

Dzurisin, Daniel, and Yamashita, K.M., 1987, Vertical surface displacements at Yellowstone caldera, Wyoming, 1976–1985: Journal of Geophysical Research, v. 92, p. 13,753–13,766.

Eaton, G.P., Christiansen, R.L., Iyer, H.M., Pitt, A.M., Mabey, D.R., Blank, H.R., Jr., Zietz, Isidore, and Gettings, M.E., 1975, Magma beneath Yellowstone National Park: Science v. 188, p. 787–796.

Farnes, P.E., 1997, The snows of Yellowstone: Yellowstone Center for Resources, Yellowstone Science, v. 5, p. 8–11.

Feng, Xiahong, and Epstein, Samuel, 1993, An [A] D/H ratio time series (1000–8000 BP) from bristlecone pine, White Mountains, California—climatic implications [abs.]: Geological Society of America Programs with Abstracts, v. 25, no. 6, p. A-256.

Ferronsky, V.I., Vlasova, L.S., Esikov, A.D., Polyakov, V.A., Seletsky, Y.B., Punning, Y.M.K., and Vajkmyaeh, R.A., 1983, Relationships between climatic changes and variations in isotopic composition of groundwater, precipitation, and organic soil matter in the Quaternary Period, *in* Paleoclimates and paleowater, a collection of environmental isotope studies: Vienna, International Atomic Energy Agency, p. 13–25.

Fournier, R.O., 1989, Geochemistry and dynamics of the Yellowstone National Park hydrothermal system: Annual Reviews Earth Planetary Sciences, v. 17, p. 13–53.

Fournier, R.O., 1991, The influences of depth of burial and the brittle-plastic transition on the evolution of magmatic fluid [abs.], *in* Hedenquist, J.W., ed., Magmatic contributions to hydrothermal systems, Extended Abstracts: Japan-U.S. seminar on magmatic contributions to hydrothermal systems, p. 43–44.

Fournier, R.O., 2000, Hydrothermal processes related to movement of fluid from plastic into brittle rock in the magmatic-epithermal environment: Economic Geology, v. 94, p. 1,193–1,212.

Fournier, R.O., and Pitt, A.M., 1985, The Yellowstone magmatic-hydrothermal system, *in* Stone, Claudia, ed., International symposium on geothermal energy: United States, Geothermal Research Council, International Volume, p. 319–327.

Friedman, Irving, Redfield, A.C., Schoen, Beatrice, and Harris, J.L., 1964, The variation of the deuterium content of natural waters in the hydrologic cycle: Reviews of Geophysics, v. 2, p. 177–224.

Fritz, Peter, 1981, River waters, *in* Gat, J.R., and Gonfiantini, R., eds., Stable isotope hydrology deuterium and oxygen-18 in the water cycle: Vienna, International Atomic Energy Agency, Technical Report Series no. 210, p. 177–202.

Gat, J.R., 1981, Groundwater, *in* Gat, J.R., and Gonfiantini, R., eds., Stable isotope hydrology, deuterium and oxygen-18 in the water cycle: Vienna, International Atomic Energy Agency, Technical Report Series no. 210, p. 223–240.

Gooch, F.A., and Whitfield, J.E., 1888, Analyses of water of the Yellowstone National Park, with an account of the methods of analysis employed: U.S. Geological Survey Bulletin 47, 84 p.

Hayden, F.V., 1872, Preliminary report of the United States Geological Survey of Montana and portions of adjacent territories, being a fifth annual report of progress, Part I: Washington, D.C., U.S. Government Printing Office, p. 13–204.

Hermann, A., Martinec, J., and Stichler, W., 1978, Study of snowmelt-runoff components using isotope measurements, *in* Colbeck, S.C., and Ray, M., eds., Modeling of snow cover runoff: Hanover, N.H., U.S. Army Cold Regions Research and Engineering Laboratory, p. 228–265.

Hildreth, Wes, Christiansen, R.L., and O'Neil, J.R., 1984, Catastrophic isotopic modification of rhyolitic magma at times of caldera subsidence, Yellowstone Plateau volcanic field: Journal of Geophysical Research, v. 89, p. 8,339–8,369.

Holdahl, S.R., and Dzurisin, Daniel, 1991, Time-dependent models of vertical deformation for the Yellowstone-Hebgen Lake region, 1923–1987: Journal of Geophysical Research, Part B, v. 96, p. 2,465–2,483.

Kendall, Carol, and Coplen, T.B., 1991, Identification of vapor-source effects versus local environmental effects on the delta D and delta O^{18} compositions of stream samples in the USA [abs.]: Geological Society of America Abstracts with Programs, v. 23, no. 5, p. A269–270.

Kendall, Carol, and Coplen, T.B., 2001, Distribution of oxygen-18 and deuterium in river waters across the United States: Hydrological Processes, v. 15, p. 1,363–1,393.

Kennedy, B.M., Reynolds, J.H., Smith, S.P., and Truesdell, A.H., 1987, Helium isotopes, Lower Geyser Basin, Yellowstone National Park: Journal of Geophysical Research, Part B, v. 92, p. 12,477–12,489.

Kennedy, B.M., Reynolds, J.H., and Smith, S.P., 1988, Noble gas geochemistry in the thermal springs: Geochimica et Cosmochimica Acta, v. 52, p. 1,919–1,928.

Lister, C.R.B., 1974, On the penetration of water into hot rock: Royal Astronomical Society Geophysical Journal, v. 39, p. 465–509.

Lister, C.R.B., 1983, The basic physics of water penetration into hot rock, *in* Rona, P.A., Bostrom, K., Laubier, L., and Smith, K.L., Jr., eds., Hydrothermal processes at seafloor spreading centers: New York, Plenum Press, p. 141–168.

Norton, D.R., and Friedman, Irving, 1991, Chloride flux and surface water discharge out of Yellowstone National Park, 1982–1989: U.S. Geological Survey Bulletin 1959, 42 p.

Patterson, W.S.B., 1981, The physics of glaciers (2d ed.): New York, Pergamon International Library of Science, Technology, Engineering and Social Studies, 380 p.

Pearson, F.J., Jr., and Truesdell, A.H., 1978, Tritium in the waters of the Yellowstone National Park, *in* Zartman, R.E., ed., Short papers of the Fourth International Conference—Geochronology, cosmochronology, isotope geology: U.S. Geological Survey Open-File Report 78-701, p. 327–329.

Pierce, K.L., 1979, History and dynamics of glaciation in the northern Yellowstone National Park area: U.S. Geological Survey Professional Paper 729-F, 90 p.

Pierce, K.L., Adams, K.D., and Sturchio, N.C., 1991, Geologic setting of the Corwin Springs Known Geothermal Resources Area–Mammoth Hot Spring Area in and adjacent to Yellowstone National Park, *in* Sorey, M.L., ed., Effects of potential geothermal development in the Corwin Springs Known Geothermal Resource Area, Montana, on the thermal features of Yellowstone National Park: U.S. Geological Survey Water Resources Investigations Report 91-4052, p. C1–C37.

Pierce, K.L., Cannon, K.P., and Meyer, G.A., 1997, Yellowstone caldera "heavy breathing" based on Yellowstone Lake and River changes in the postglacial time: Eos, Transactions, American Geophysical Union, v. 78, no. 46, p. F802.

Pitt, A.M., 1987, Tectonics of the Hebgen Lake–northwest Yellowstone Park region from earthquake hypocenters and focal mechanisms: Seismological Research Letters, v. 58, 29 p.

Rye, R.O., and Truesdell, A.H., 1993, The question of recharge to the geysers and hot springs of Yellowstone: U.S. Geological Survey Open-File Report 93-384, 40 p.

Smith, G.I., Friedman, Irving, Guida, Veronda, and Johnson, C.A., 2002, Stable isotope compositions of water in the Great Basin, United States, Part 3—Comparison of ground waters with modern precipitation: Journal of Geophysical Research, v.107, no. D19, p. ACL 1–16.

Smith, R.B., and Rubin, A.M., 1994, Rapid reversals of uplift to subsidence at the Yellowstone caldera by magmatic processes imaged by earthquakes: Seismological Research Letters, v. 65, p. 56.

Sorey, M.L., ed., 1991, Effects of potential geothermal development in the Corwin Springs Known Geothermal Resource Area, Montana, on the thermal features of Yellowstone National Park: U.S. Geological Survey Water-Resources Investigations Report 91-4052, 193 p.

Sorey, M.L., Lewis, R.W., and Olmsted, F.H., 1978, The hydrothermal system of Long Valley caldera, California: U.S. Geological Survey Professional Paper 1044-A, 60 p.

Taylor, H.P., Jr., 1986, Igneous rocks II—Isotopic case studies of circumpacific magmatism, *in* Valley, J.W., Taylor, H.P., Jr., O'Neil, J.R., eds., Stable isotopes in high temperature geological processes: Reviews in Mineralogy, v. 16, p. 273–318.

Thordsen, J.J., Kharaka, Y.K., Mariner, R.H., and White, L.D., 1992, Controls on the distribution of stable isotopes of meteoric water and snow in the greater Yellowstone National Park region, USA, *in* Kharaka, Y.K., and Maest, A.S., eds., Water-rock interaction: Rotterdam, Balkema, p. 591–595.

Truesdell, A.H., and Fournier, R.O., 1976, Conditions in the deeper parts of hot spring systems of Yellowstone National Park: U.S. Geological Survey Open-File Report 76-428, 29 p.

Truesdell, A.H., Nathenson, Manuel, and Rye, R.O., 1977, The effects of subsurface boiling and dilution on the isotopic compositions of the Yellowstone thermal waters: Journal of Geophysical Research, v. 82, p. 3,694–3,704.

Vance, R.E., Mathews, R.W., and Clague, J.J., 1992, 7,000 year record of lake-level change on the northern Great Plains—A high-resolution proxy of past climate: Geology, v. 20, p. 879–882.

Whitlock, Cathy, 1993, Postglacial vegetation and climate of the Grand Teton and southern Yellowstone National Parks: Ecological Monographs, v. 63, p. 173–198.

Wicks, Charles, Jr., Thatcher, Wayne, and Dzurisin, Daniel, 1999, Migration of fluids beneath the Yellowstone caldera inferred from satellite radar interferometry: Science, v. 282, p. 485–461.

White, A.F., Chuma, N.J., and Goff, Frazer, 1992, Mass transfer constraints on the chemical evolution of an active hydrothermal system, Valles caldera, New Mexico: Journal of Volcanology Geothermal Research, v. 49, p. 233–253.